Making Precision Measurements at Hadron Colliders

Henry Frisch

University of Chicago

Lake Louise Winter Institute, Feb. 17-23, 2006

Contents

Lecture I: The Electroweak Scale: Top, the W and Z, and the Higgs via M_W and M_{top}

1 Introduction: Purpose

These two lectures are purely pedagogical. My intent is to enable non-experts to get something out of the individual presentations on collider physics that will follow- the Higgs, the W,Z, top, searches for SUSY, LED's, etc. We are presented with so many measurements and so much detail that we often forget that we are talking about instruments and the measurements they have made. The suprise is how precise the detectors themselves are; the challenge will be to exploit that precision in the regime where statistics is no longer a problem, and everything is dominated by the performance of the detector ('systematics').

This challenge also extends to the theoretical community- to look for something new we will need to understand the non-new, i.e. the SM predictions, at an unprecedented level of precision. Some amount of this can be done with control samples- it is always best to use data rather than Monte Carlo, but it's not always possible. The detectors are already better than the theoretical predictions- the theory community needs to catch up.

Problems in Making Precision Measurements

The emphasis here will be more on problems to be addressed than on new results. I work on CDF, and have used mostly CDF plots just because I know the details better- the problems however are more general. No slight to DØ or the LHC experiments is meant. I have cut some corners in places and been a little provocative in others, as teachers will. All views presented here are my own, as is the amateur presentation.

I have intentionally used older public results from CDF and *DØ* instead of the hot-off-the-press results generated for the 2006 'winter conferences' so as not to steal the thunder of the invited speakers who are here to present new results from CDF and D0. The idea is to provide the understanding so that you can recognize the evolution of the results, ask the hard questions, and to provoke discussion. This is going to be really different from a raporteur's talk...

2 Some History and Cultural Background

2.1 Luminosity History: Orders of Magnitude

A brief history of luminosity, starting with the $SP\bar{P}S$ and the race to discover the W and the Z^0, and then the race to discover the top, is shown in Figure 1.

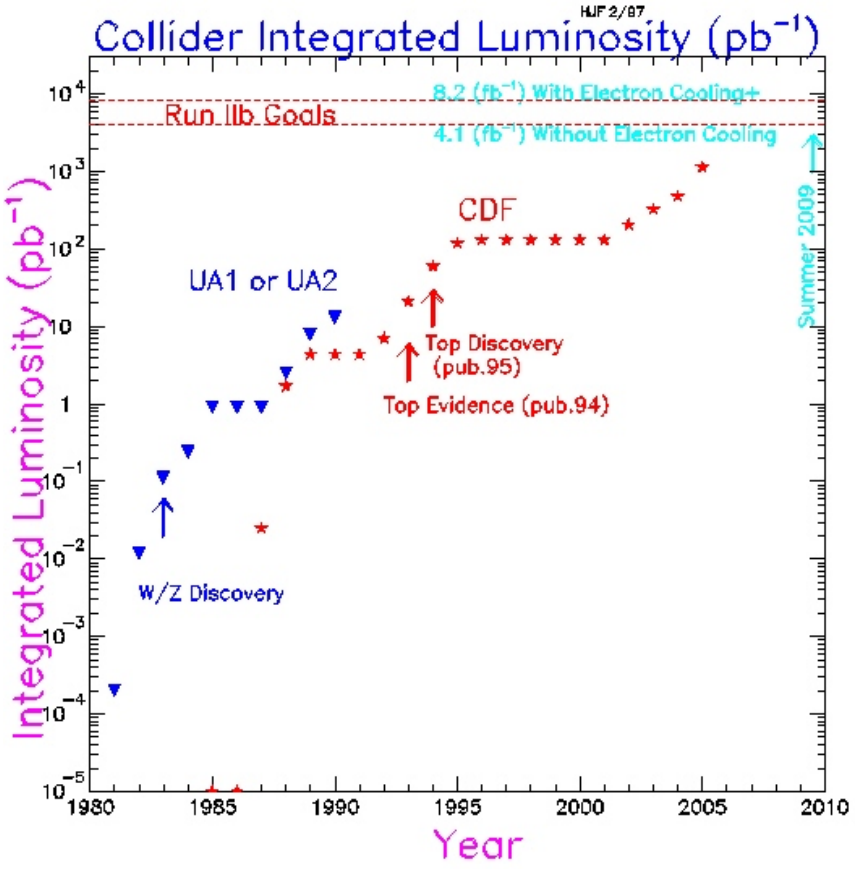

Figure 1: A history of high-energy (no ISR) hadron colliders: integrated luminosity by year.

’88: Inverse Nanobarns ’06: Inverse Femtobarns

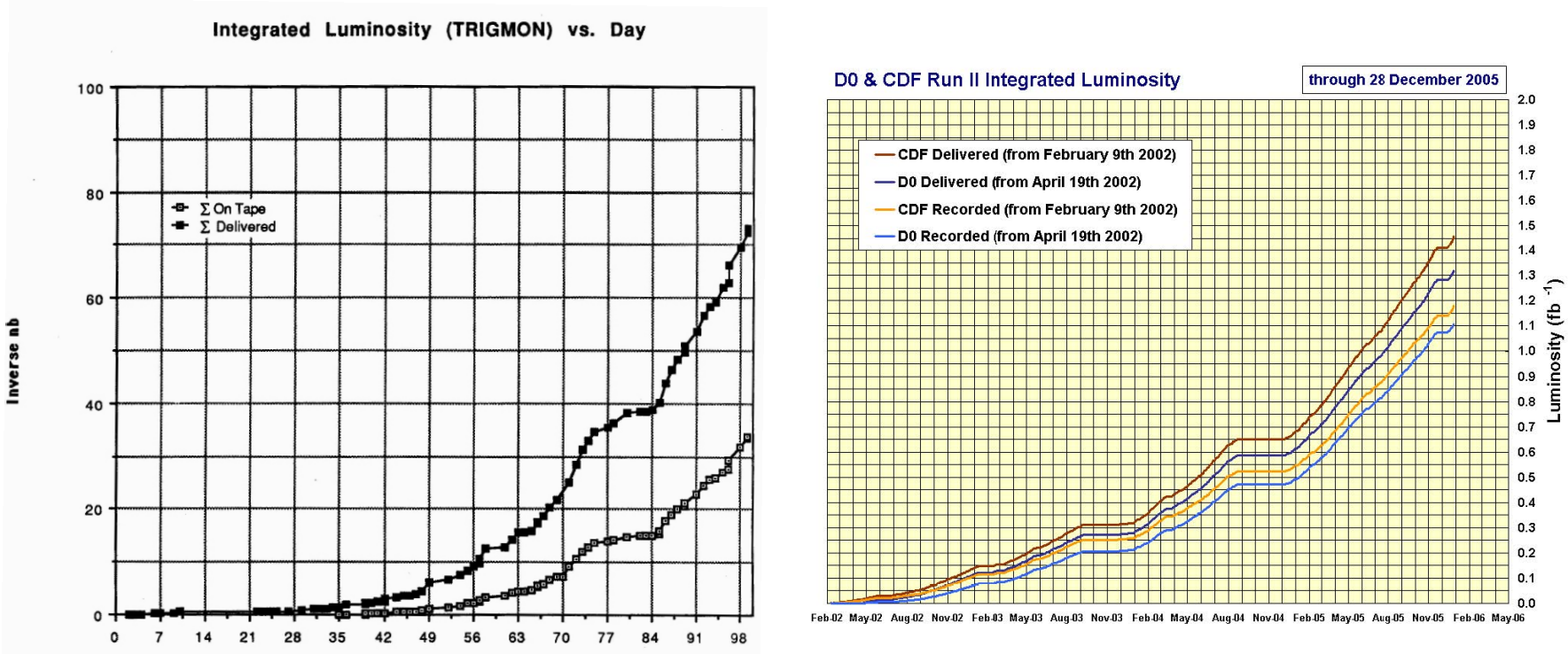

Figure 2: The integrated luminosity in the 1987 Tevatron run (Left), in Inverse Nanobarns, and in Run II (Right), in Inverse Femtobarns. Note that 1 fb^{-1}= 10^3 pb^{-1}= 10^6 nb^{-1}. Note also the efficiency for tape (beginning Feb. 1, 1987) improved substantially.

Figure 2 shows the luminosity ‘delivered’ and ‘to tape’ from the current Run II, in inverse femtobarns (right), and from the 1987 run, in inverse nanobarns. As a quick reminder, the $W^{\pm} \rightarrow e^{\pm}\nu$ cross-section times BR is about 2.2 nb for the left-hand plot, so 30 nb^{-1}means that 66 $W^{\pm} \rightarrow e^{\pm}\nu$ decays were created in the recorded exposure. The cross-section for a 115 GeV Higgs in $W^{\pm} \rightarrow e^{\pm}\nu + H$ production is $\sim$20 fb, and so the right hand plot indicates that 20 $W^{\pm} \rightarrow e^{\pm}\nu + H$ events were created in 1fb^{-1}at either DØ or CDF.

2.2 Hubris: The 50 GeV Top Quark and No Quarkonia

Figure 3 (on next page) is an historical reminder both that we should not be over-confident about what we know, and that Nature has a rich menu of surprises. The left-hand page is the discovery of something that did not exist- a top quark with mass less than 50 GeV (it was largely W+jets, as shown by Steve Ellis). The right-hand page is a prediction that there are no narrow states with masses between 3 and 10 GeV decaying into lepton pairs (note both these guys did well- they kept looking, and Nature gave them both more chances!).

(Tell Lederman, Richter and Rubbia story if there's time... or a question.)

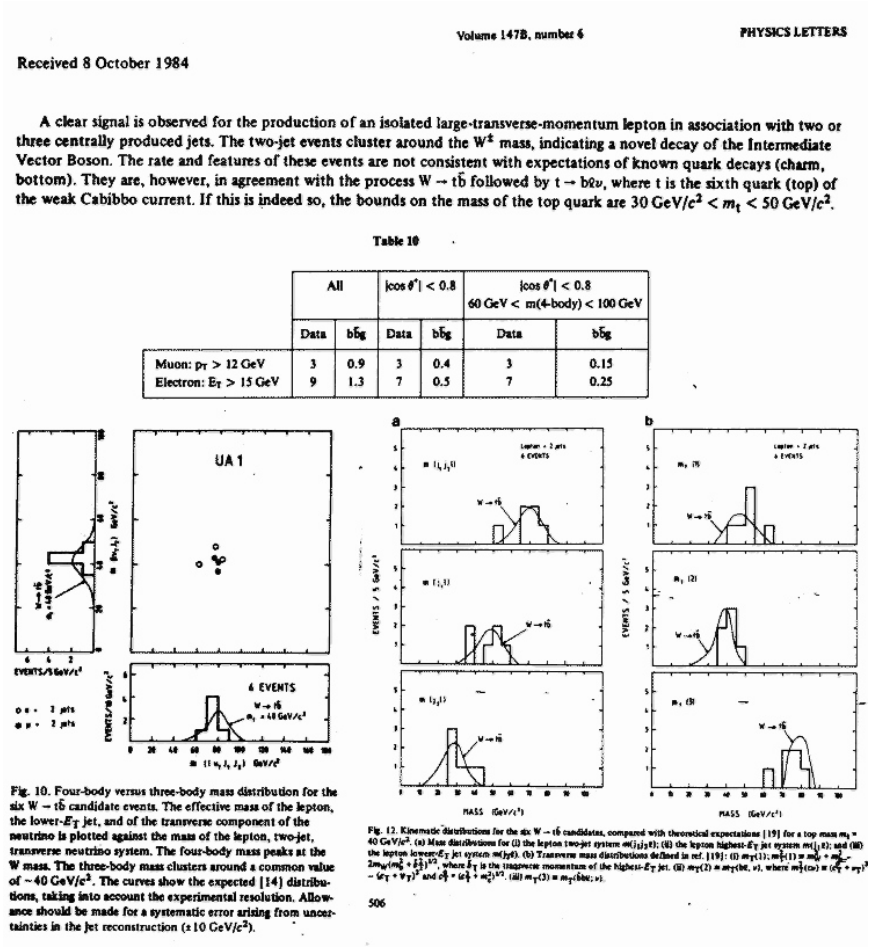

Volume 147B, number 6 PHYSICS LETTERS

Received 8 October 1984

A clear signal is observed for the production of an isolated large-transverse-momentum lepton in association with two or three centrally produced jets. The two-jet events cluster around the $W^{\pm}$ mass, indicating a novel decay of the Intermediate Vector Boson. The rate and features of these events are not consistent with expectations of known quark decays (charm, bottom). They are, however, in agreement with the process $W \to t\bar{b}$ followed by $t \to b\ell\nu$, where t is the sixth quark (top) of the weak Cabibbo current. If this is indeed so, the bounds on the mass of the top quark are $30\ \mathrm{GeV}/c^2 < m_t < 50\ \mathrm{GeV}/c^2$.

Table 10

	All		$\lvert\cos\theta^*\rvert < 0.8$		$\lvert\cos\theta^*\rvert < 0.8$, 60 GeV < m(4-body) < 100 GeV	
	Data	$b\bar{b}g$	Data	$b\bar{b}g$	Data	$b\bar{b}g$
Muon: $p_T > 12$ GeV	3	0.9	3	0.4	3	0.15
Electron: $E_T > 15$ GeV	9	1.3	7	0.5	7	0.25

UA 1

4 EVENTS

Fig. 10. Four-body versus three-body mass distribution for the six $W \to t\bar{b}$ candidate events. The effective mass of the lepton, the lower-E_T jet, and of the transverse component of the neutrino is plotted against the mass of the lepton, two-jet, transverse neutrino system. The four-body mass peaks at the W mass. The three-body mass clusters around a common value of ~40 GeV/c^2. The curves show the expected [14] distributions, taking into account the experimental resolution. Allowance should be made for a systematic error arising from uncertainties in the jet reconstruction (± 10 GeV/c^2).

Fig. 12. Kinematic distributions for the six $W \to t\bar{b}$ candidates, compared with theoretical expectations [19] for a top mass m_t = 40 GeV/c^2. (a) Mass distributions for (i) the lepton two-jet system $m(j_1 j_2)$; (ii) the lepton highest-E_T jet system $m(j_1)$; and (iii) the lepton lowest-E_T jet system $m(j_2)$. (b) Transverse mass distributions defined in ref. [19]: (i) $m_T(1)$; $m_T^2(1) = m_{j_1}^2 + m_{j_2}^2 + 2m_{j_1}(m_{j_2}^2 + \vec{p}_{j_2}^{\,2})^{1/2} - 2\vec{p}_{j_1}\cdot\vec{p}_{j_2}$, where $\vec{p}_{j_1}$ is the transverse momentum of the highest-E_T jet. (ii) $m_T(2) = m_T(b\ell\nu, \nu)$, where $m_T^2(\alpha\nu) = (\sqrt{\vec{p}_\alpha^{\,2} + m_\alpha^2} + |\vec{p}_\nu|)^2 - (\vec{p}_\alpha + \vec{p}_\nu)^2$ and $\vec{p}_\alpha^{\,2} + m_\alpha^2 = E_\alpha^2$. (iii) $m_T(3) = m_T(b\ell\nu; \nu)$.

506

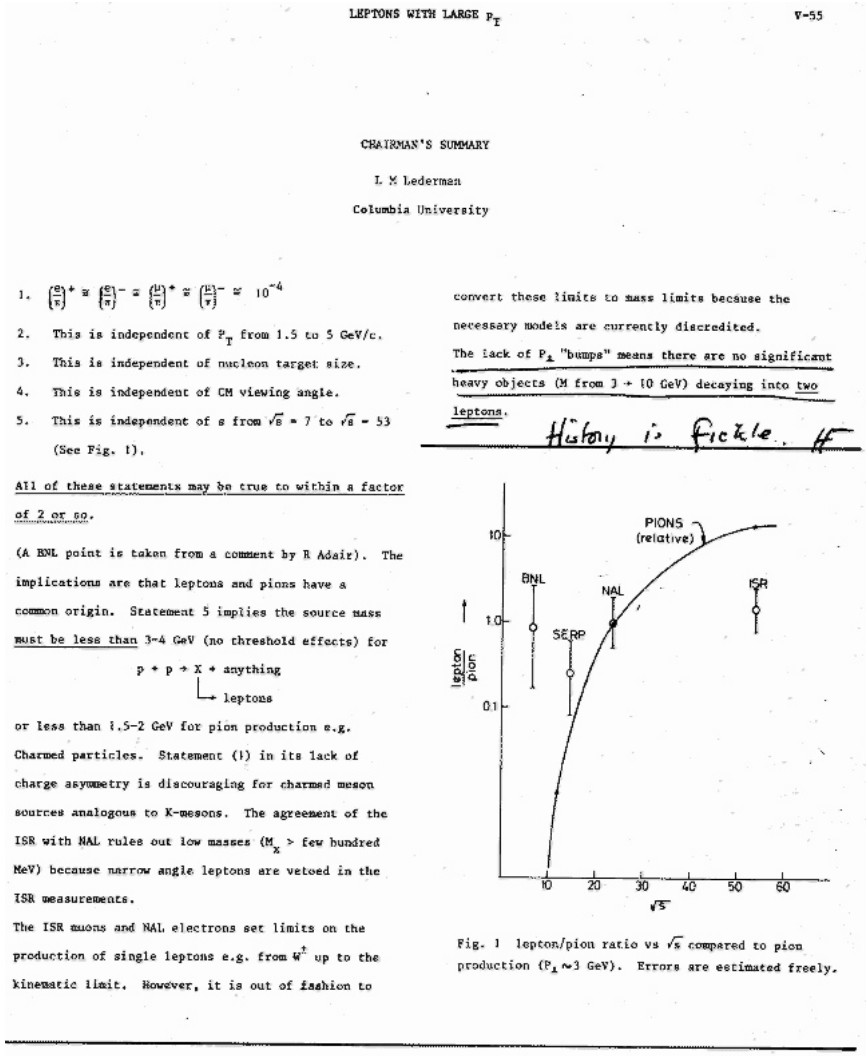

LEPTONS WITH LARGE p_T V-55

CHAIRMAN'S SUMMARY

L M Lederman

Columbia University

1. $\left(\frac{e}{\pi}\right)^+ \cong \left(\frac{e}{\pi}\right)^- \cong \left(\frac{\mu}{\pi}\right)^+ \cong \left(\frac{\mu}{\pi}\right)^- \cong 10^{-4}$
2. This is independent of P_T from 1.5 to 5 GeV/c.
3. This is independent of nucleon target size.
4. This is independent of CM viewing angle.
5. This is independent of s from $\sqrt{s} = 7$ to $\sqrt{s} = 53$ (See Fig. 1).

All of these statements may be true to within a factor of 2 or so.

(A BNL point is taken from a comment by R Adair). The implications are that leptons and pions have a common origin. Statement 5 implies the source mass must be less than 3-4 GeV (no threshold effects) for

p + p → X + anything
└→ leptons

or less than 1.5-2 GeV for pion production e.g. Charmed particles. Statement (1) in its lack of charge asymmetry is discouraging for charmed meson sources analogous to K-mesons. The agreement of the ISR with NAL rules out low masses (M_X > few hundred MeV) because narrow angle leptons are vetoed in the ISR measurements.

The ISR muons and NAL electrons set limits on the production of single leptons e.g. from $W^{\pm}$ up to the kinematic limit. However, it is out of fashion to convert these limits to mass limits because the necessary models are currently discredited.

The lack of $P_\perp$ "bumps" means there are no significant heavy objects (M from 3 + 10 GeV) decaying into two leptons.

History is fickle. HF

PIONS (relative)
BNL
SERP
NAL
ISR
lepton / pion
10
1.0
0.1
10
20
30
40
50
60
$\sqrt{s}$

Fig. 1 lepton/pion ratio vs $\sqrt{s}$ compared to pion production ($P_\perp \sim 3$ GeV). Errors are estimated freely.

Figure 3: Left: The 1984 Top 'discovery'; Right: The 1974 'no discovery' announcement of the J/ψ and Upsilons.

3 The Tevatron and the LHC

By now everybody should know about the Tevatron and LHC. I will spare you pictures and boilerplate; The main differences that everybody, including theorists, should know are:

	Tevatron	LHC
Parton Source	Antiproton-Proton	Proton-proton
Energy (TeV)	1.96 (not 2!)	14
Peak Luminosity ($\mathrm{cm}^{-2}\mathrm{s}^{-1}$)	2×10^{32}	1×10^{34}
Crossing Spacing (ns)	396	24.95
Peak Interactions/Crossing	5	19
Luminous Line σ (cm)	30	4.5 [**?**]
Luminosity Lifetime (hours)	3.8/23 [**?**]	15
$< x >$ at M_W	0.04	0.006
$< x >$ at $2M_T$	0.18	0.025

An LHC upgrade to 1×10^{35} is planned.

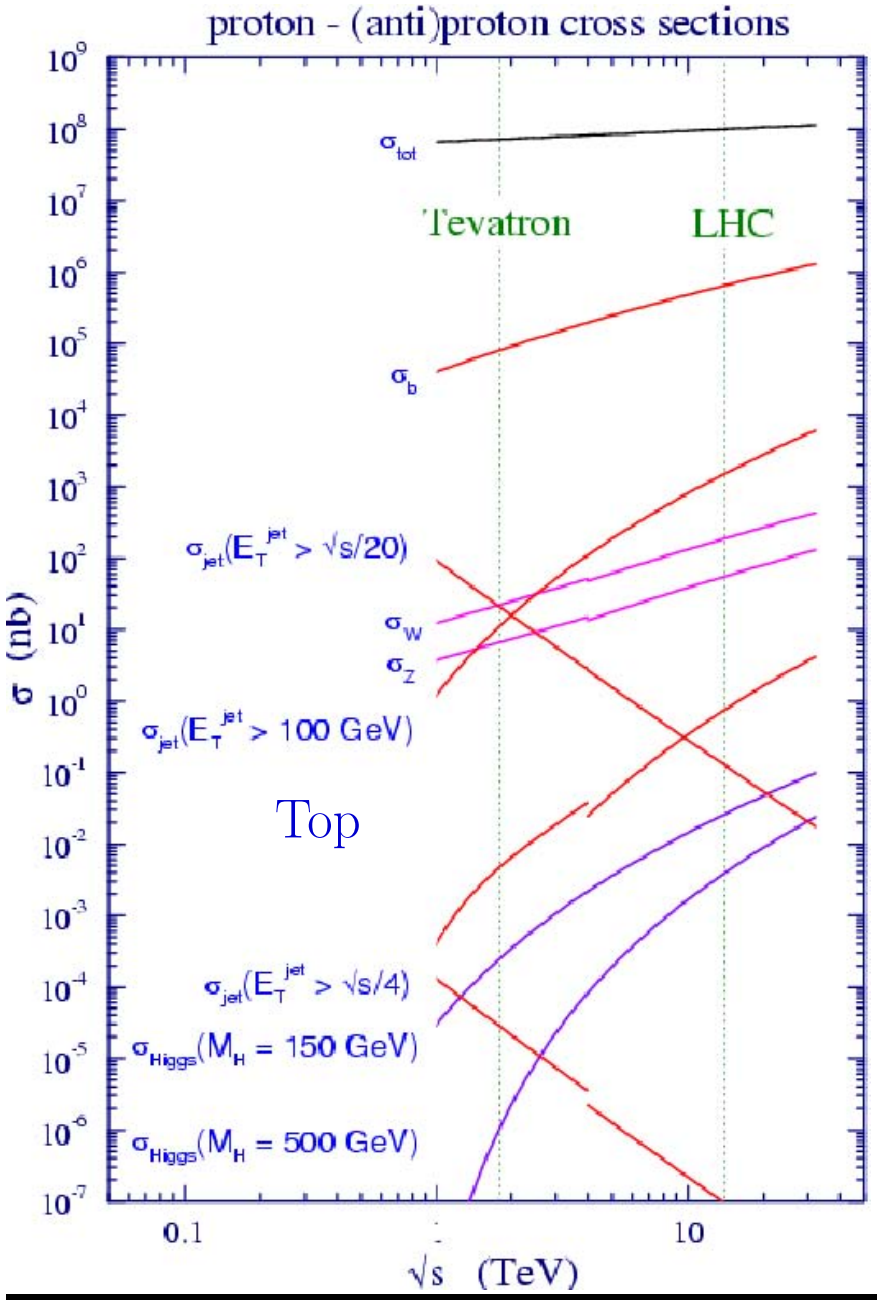

A map of useful cross-sections vs Root-s from Tevatron to LHC.

Note: 1. 16 orders-of-magnitude

2. σ_{tot} rising only logarithmically;

3. Tevatron just entering decent statistics for top (7-8000 fb);

4. Higgs cross-section is down by 12 orders-of-magnitude at the Tevatron.

4 The Anatomy of Detectors at Hadron Collider: Basics

I start with a brief elementary introduction. For those moving to the LHC from Cornell, SLAC, or LEP, working at a hadron collider is really different from at an e^+e^- machine- took a previous CDF spokesperson (un-named) from e^+e^- several years to understand 'whatever you ask for in your trigger will you get' (the story of jets at ISR and Fermilab).

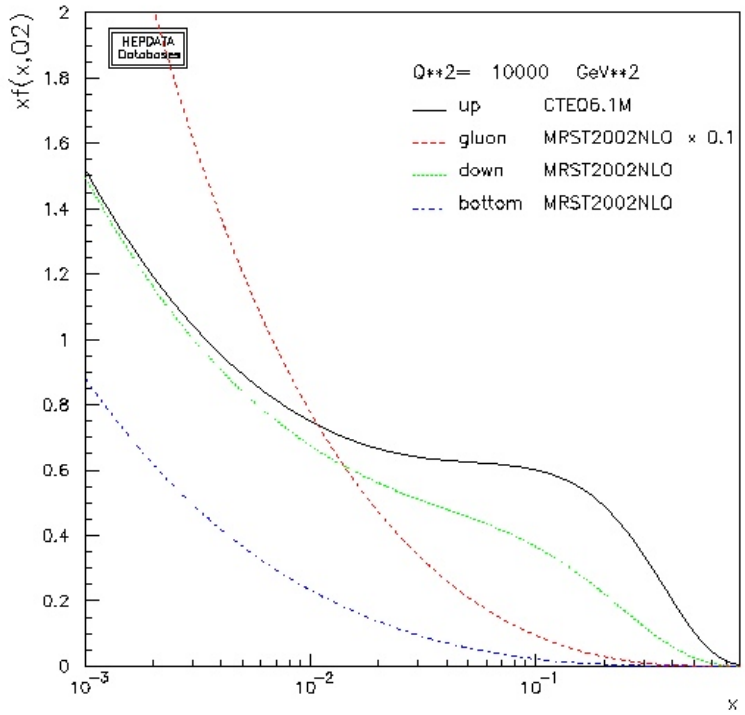

Figure 4: The CTEQ6.1M PDF's at Q=100 (Joey Huston).

4.1 Basics: Kinematics and Coverage: p_T vs $P_{||}$

The phase space for particle production at a hadron collider is traditionally described in cylindrical coordinates with the z axis along the beam direction, the radial direction called 'transverse', as in 'Transverse Momentum' (p_T), and the polar angle expressed as Pseudo-rapidity η, where $\eta \equiv -ln(tan\theta/2))$. Pseudo-rapidity is a substitute for the Lorentz-boost variable, y, where $y \equiv 1/2ln(E+p_z)/(E-p_z) \equiv tanh^{-1}(p_z/E)$. Since in most cases one does not know the mass of a particle produced in a hadron collision (most are light- pions, kaons, baryons,..), we use pseudo-rapidity. (This is a common trap when doing complex kinematics with W's, Z's, and top, where the mass truly matters). Figure 5 shows an early sketch of the proposed coverage in η for CDF; note that the big central detector seems very small, while the little luminosity monitors seem big. Note that typical particle production is 4-6 particles per unit-rapidity; in the central region one unit at CDF is about 14 m^2; the density in a min-bias event is very low. Hadron colliders are not intrinsically 'dirty'- only complex.

Each beam-beam counter was about .75 in η- closest to beam pipe was 2 cm across. 1.0 in η in central is about 1.5m.

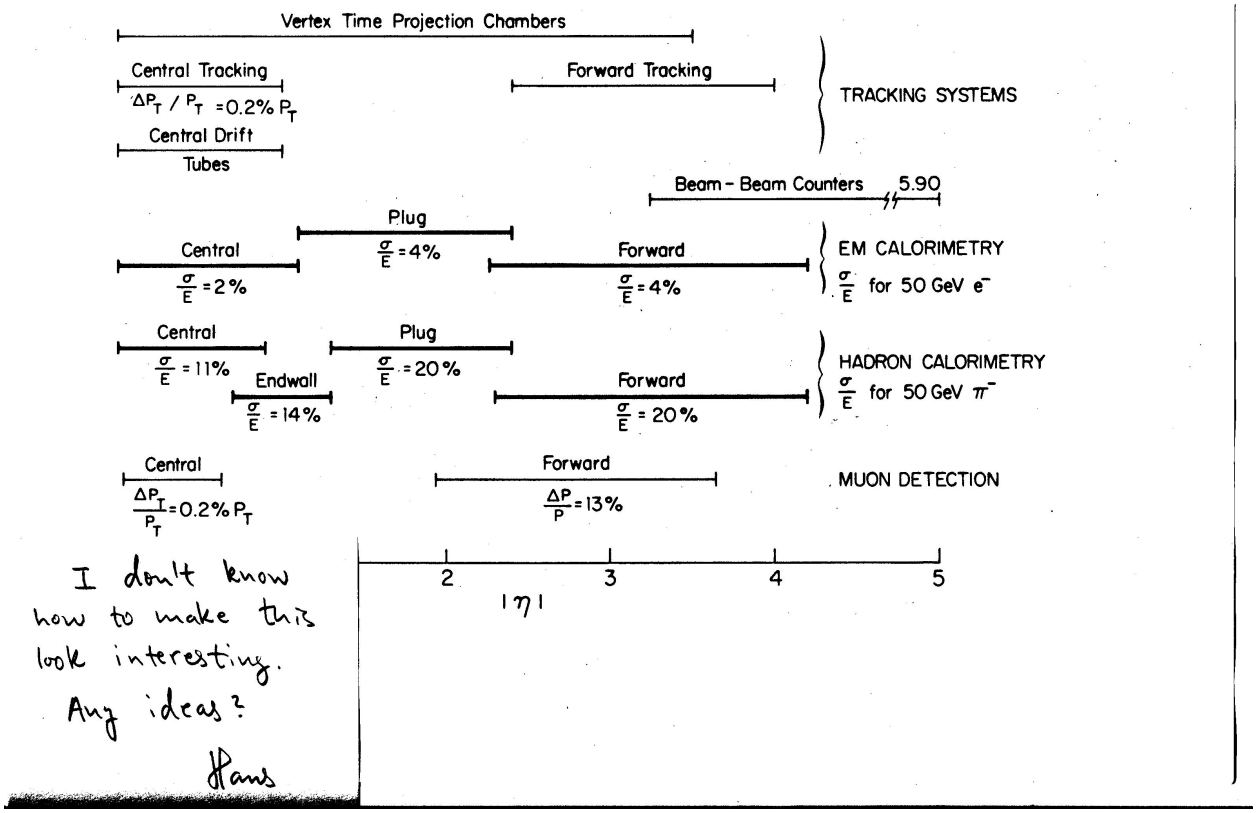

Figure 5: An early planning document (Hans Jensen) for the coverage in rapidity for CDF (ans- no way to make it look interesting, but..)

Two simple equations contain much of the physics for the production of heavy states at a collider: the mass and longitudinal momentum of the heavy state (e.g. a W, Z, $t\bar{t}$ pair, or WH) are determined by the fraction of the beam momentum carried by the interacting partons. Note that for a heavy object typically has a velocity $\beta << 1$, even though the longitudinal momentum is typically not small (we're not in the c.m! of the collision.). Note also that the transverse momentum of the system is determined by the competition of falling parton distribution functions (PDF's- also known as structure functions) as the total invariant mass of the system rises, and the increase in phase space as the momentum of the system increases. The production thus peaks with a total system energy above threshold by an amount characteristic of the slope in $x_1 * x_2$.

$$m^2 = x_1 * x_2 s \qquad\qquad p_z = (x_1 - x_2) p_{beam} \tag{1}$$

4.2 Basics: Particle Detection

While low-momentum– typically up to a few GeV– charged particles can be identified by processes that depend on their velocity, β, as a simultaneous measurement of $p = \beta\gamma m$ and β allows extracting the mass, for momenta above a few GeV, pions, kaons, and protons cannot be separated. However electrons, muons, hadrons, and neutrinos interact differently, as shown in Figure 4.2. The measurement of their energies and/or momenta stem from their different modes of interaction.

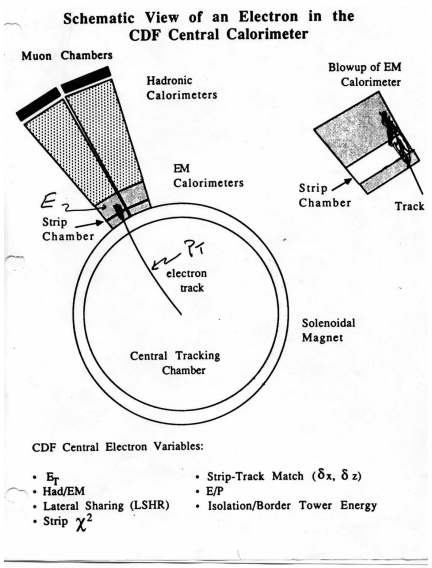

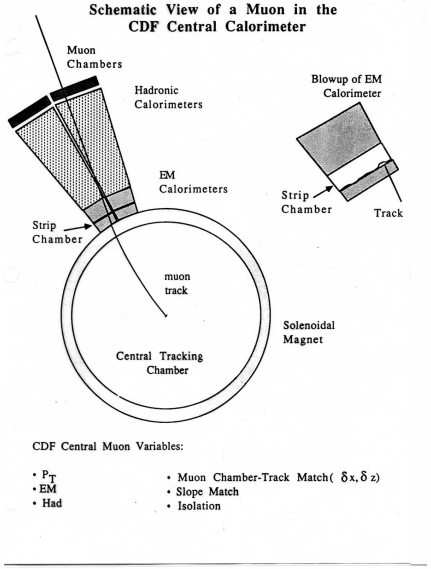

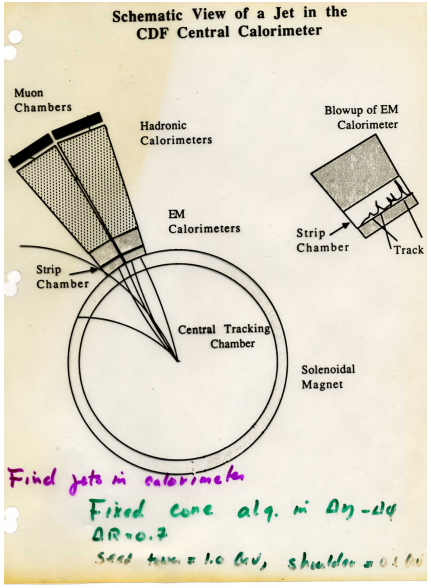

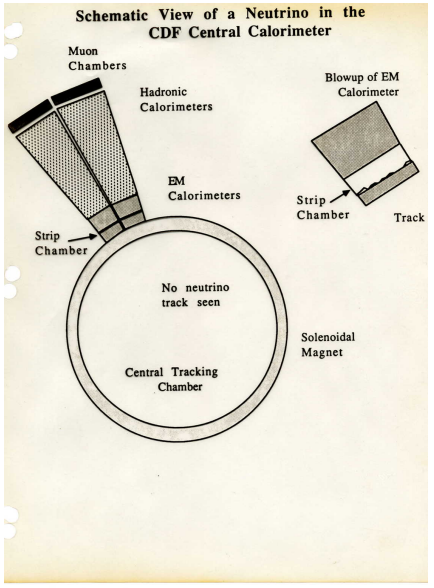

5 Calibration Techniques

5.1 Momentum and Energy Scales: E/p

The Tevatron and the LHC are as different from LEP and other e^+e^- colliders as night and day- it is a big disadvantage to have worked at LEP(!). One key difference is that the overall mass (energy) scale is not set by the beam energy- there is a continuum of c.m. energies in the parton-parton collisions. Moreover the hard scattering is not at rest either longitudinally *nor* transverse in the lab system- there is 'intrinsic Kt' as well as initial-state radiation (ISR). Finally, the beam spot is a line and not a spot- the vertex point, used to calculate transverse energies, has to be determined from the event, including for neutrinos and photons for which no track is observed.
Dealing first with the issue of setting the scale for momentum, energy, and mass measurements. All current detectors consist of a magnetic spectrometer followed by calorimeters. The magnetic spectrometer uses a precisely measured (NMR) magnetic field and the precise geometry of the tracking chambers to measure the curvature $(1/P_T)$of the tracks of charged particles. This is an absolute measurement- if perfect one has the momentum scale. One can then use particles with measured momentum as an *in situ* 'test beam' to calibrate the energy scale of the calorimeters.

The momentum scale can be checked by measuring the masses of some calibration 'lines' thoughtfully provided by Mother Nature- the J/Psi and Υ systems, and the Z^0in its $Z^0 \to \mu^+\mu^-$ decays ($Z^0 \to e^+e^-$ doesn't work for momentum calibration!). Fig. 6 shows measured distributions from CDF. However the momentum scale can be incorrect due

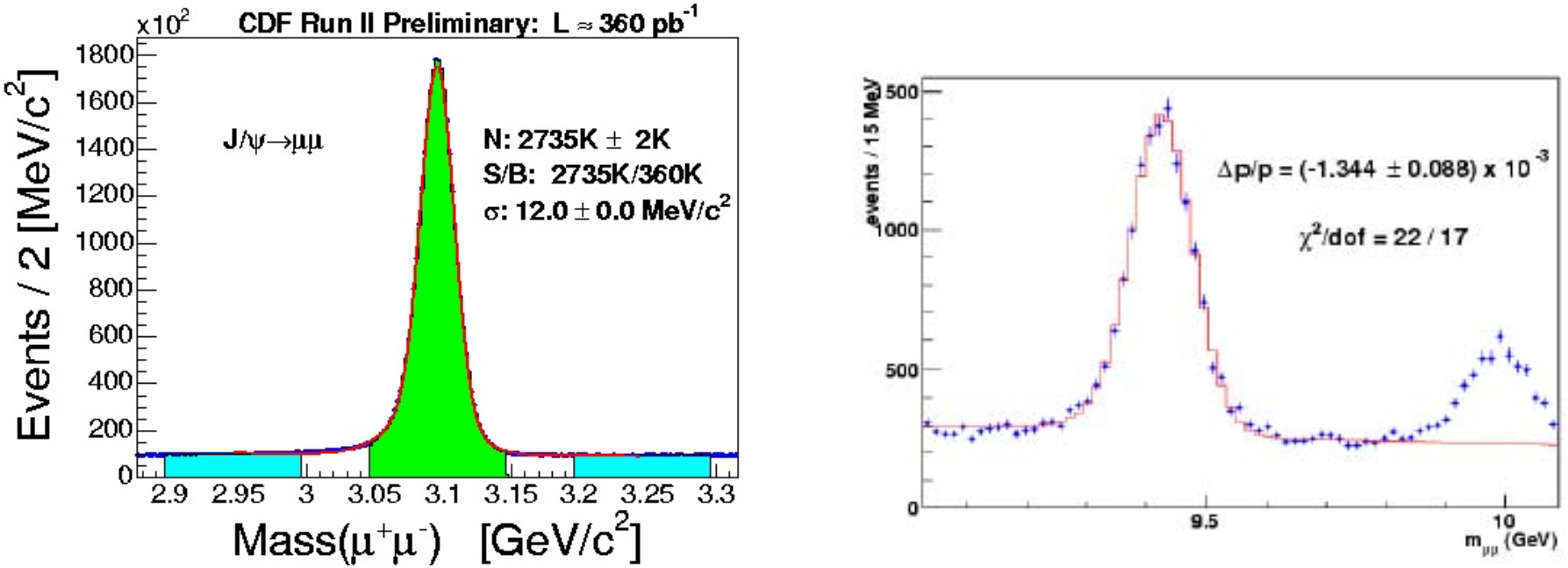

Figure 6: Left: The reconstructed $J\Psi$ invariant mass in dimuons (CDF). Right: The similar plot for the Upsilon system.

to mis-alignments in the tracking chamber. The combination of a calorimeter and a magnetic spectrometer allows one to remove the 1st-order errors in both [**?**] by measuring 'E' (calorimeter energy) over 'p' (spectrometer moementum. With perfect resolution,

no energy loss, and no radiation these two should be equal: $E/p = 1.0$. Figure 7 shows the measured spectrum in E/p for electrons.
The 1st-order error in momentum is due to a 'false-curvature'- that is that a straight line (zero-curvature= ∞ momentum) is reconstructed with a finite momentum. The 1st-order error in calorimeter energy is an offset in the energy scale, and does not depend on the sign ($\pm$) of the particle [**?**]. Expanding both the curvature and calorimeter energies to first order:

$$1/p = 1/p_{true} + 1/p_{false} \quad (\mu^+) \quad 1/p = 1/p_{true} - 1/p_{false} \quad (\mu^-) \tag{2}$$

$$E = E_{true} * (1 + \epsilon) \quad (e^+) \quad E = E_{true} * (1 - \epsilon) \quad (e^-) \tag{3}$$

The first-order false curvature p_{false} then is derived by measuring E/p for positive and negative electrons with the same E

$$1/p_{false} = ((E/p(e^+) - E/p(e-))/2E \tag{4}$$

The first-order calibration scale error ϵ then is removed by setting the calorimeter scale for electrons so that E/p agrees with expectations. In CDF, this is done initially to make the calorimeter response uniform in $\phi - \eta$.

$$1/p_{false} = ((E/p(e^+) + E/p(e-))/2 \tag{5}$$

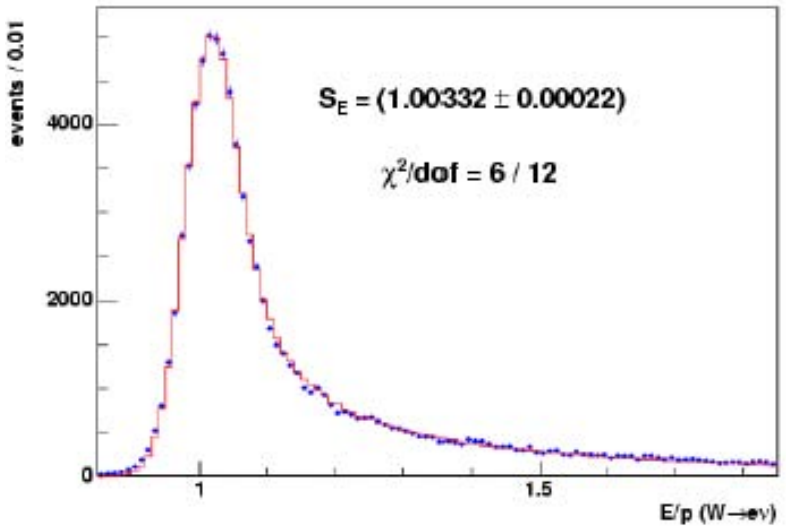

Figure 7:

5.2 Higher-order momentum and energy corrections

The momentum and energy calibrations at this point are good enough for everything at present exposures except the W mass measurement. There are three higher-order effects that are taken care of at present:

1. 'Twist' between the 2 end-plates of the tracking chamber;
2. Systematic scale change in the z-measurements in the chamber;
3. Non-linearity of the calorimeter due to $e(E/2) + \gamma(E/2) \neq e(E)$

Figure 8 shows the use of the J/Ψ mass to correct for the first two of these effects. What is plotted is the correction to the momentum scale versus the cotan of the difference in polar (from the beam axis) angle of the two muons. There is a linear correction to the curvature of $\delta c = 6 \times 10^{-7} cot(\theta)$ that corrects for the twist between the endplates, and a change in the scale of the z-coordinate by 2 parts in 10^4, $z_{scale} = 0.9998 \pm 0.0001$. This is precision tuning of a large but exceptionally precise instrument!

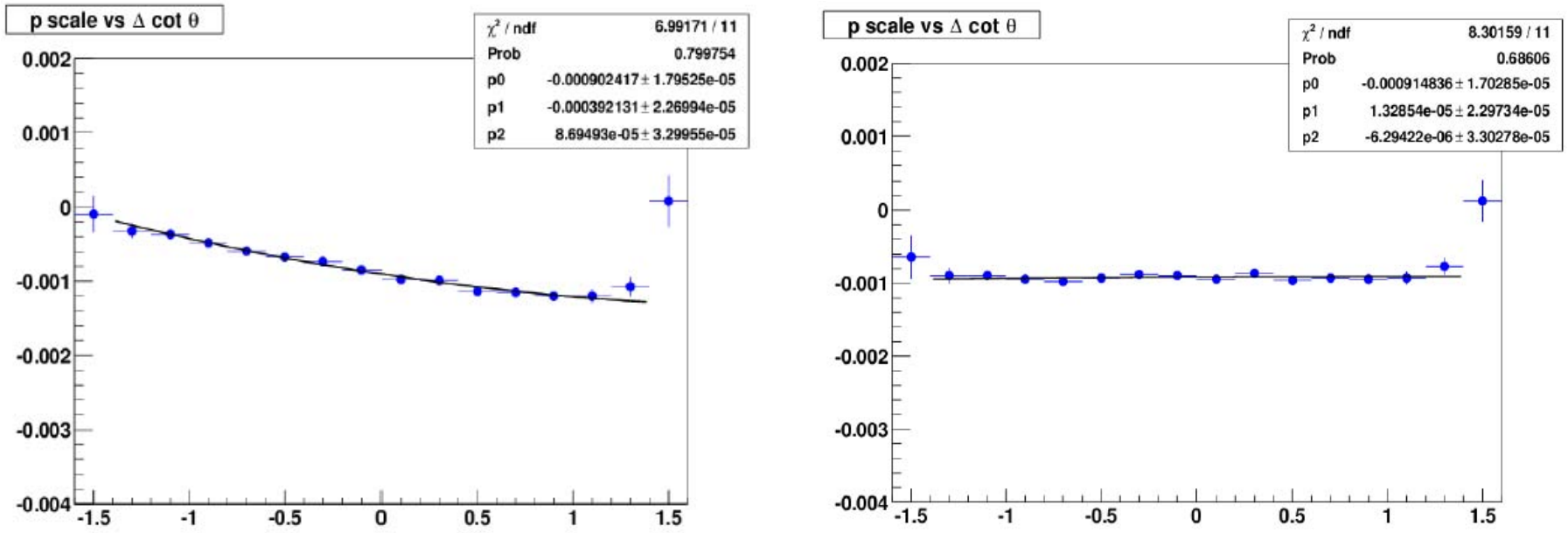

Figure 8: Left: The correction to the momentum scale versus the cotan of the difference in polar angle of the two muons in J/psi decay before corrections: Right: The same after correcting the curvature by $\delta c = 6 \times 10^{-7} cot(\theta)$ the scale of the z-coordinate by 2 parts in 10^4.

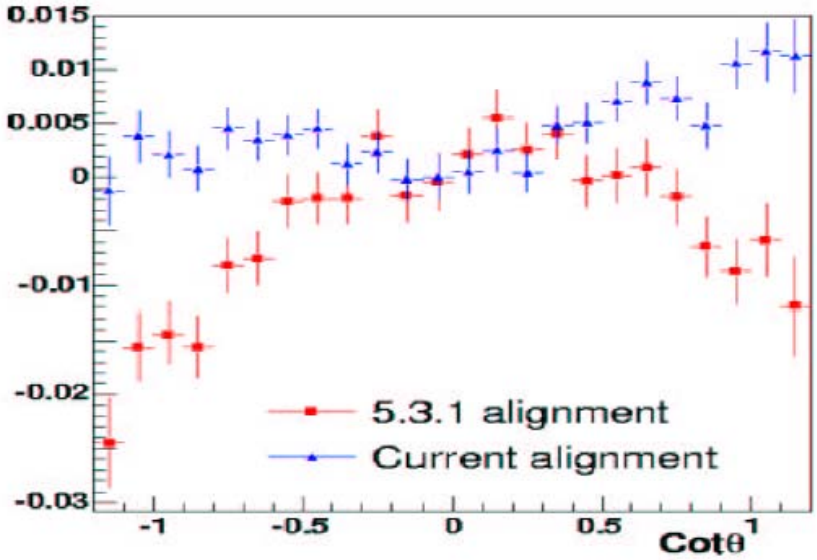

Figure 9: Measuring a higher-order correction to track curvature: the calorimeter to momentum ratio E/p versus $cot\theta$ for e^+ and e^-, before and after the curvature and z-scale corrections.

5.3 Calibrating the Hadron Calorimeters and the Jet Energy Scale

Much of the top mass information is encoded in its jets: the b-jets are first-generation daughters of a 2-body decay, one W decays into 2 jets, and the missing-Et of the neutrino is measured in the calorimeter.
There are a number of ways to calibrate the calorimeter response to jets:

1. In situ calibration by isolated hadrons ('E/p')
2. Test beam (for higher momenta- but, remember UA2- long ago for CDF
3. Dijet balancing (D0 uses this cleverly at large η for Et reach0
4. γ-jet balancing
5. Z^0-jet balancing

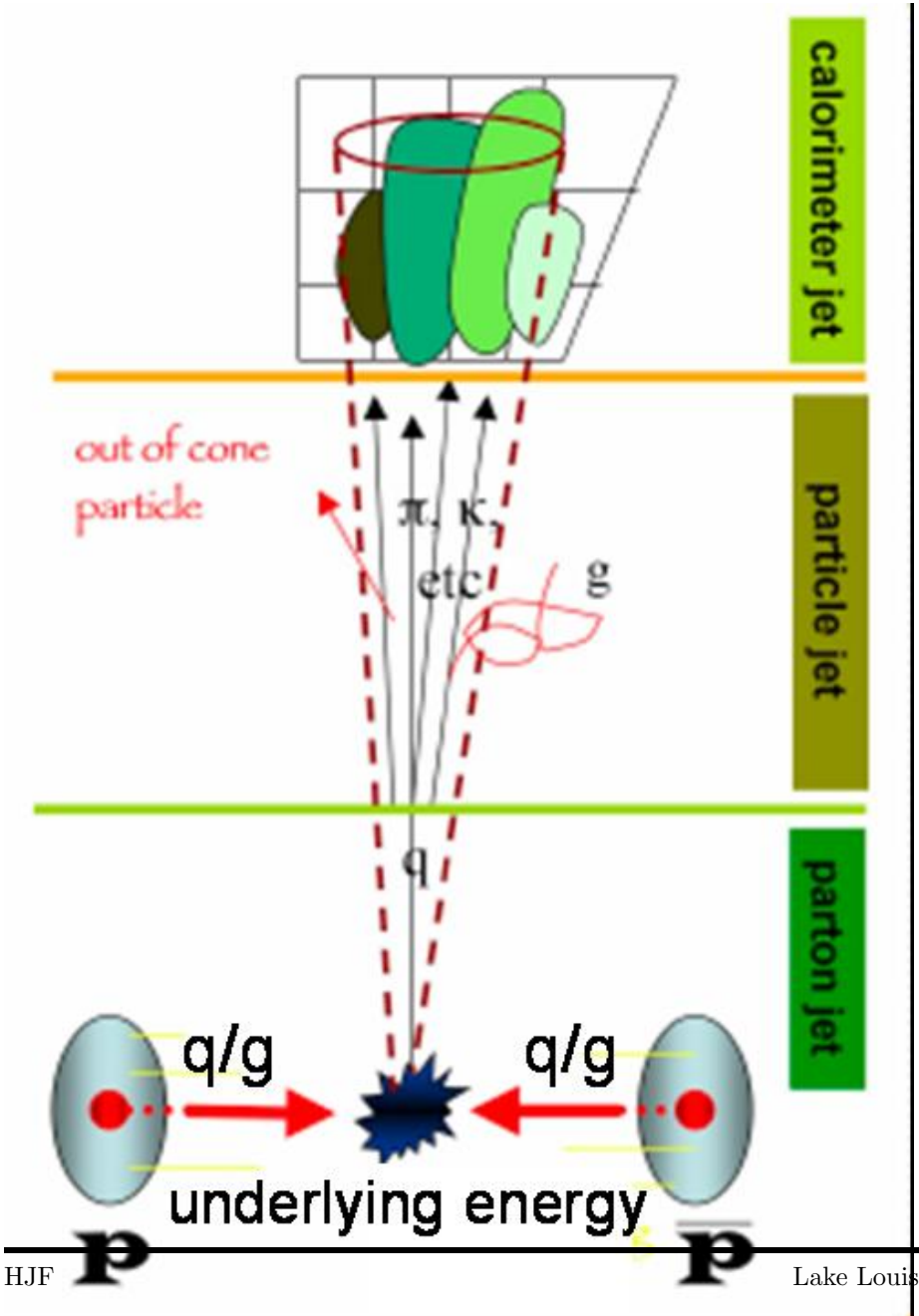

The total Uncertainties on the jet energy scale.

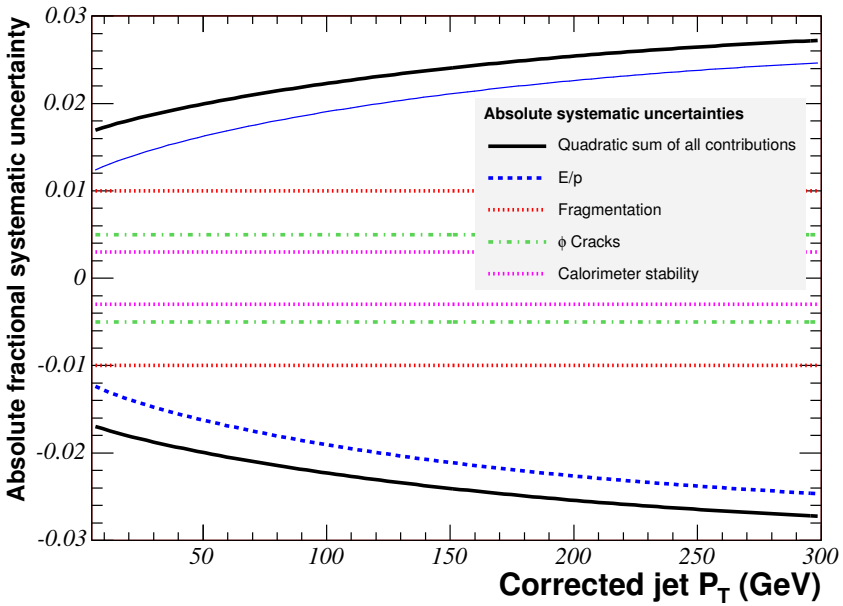

After much hard work, check 'relative' (flat in η) calibrations with gamma-jet balancing: photon on one side should balance a jet on the other.

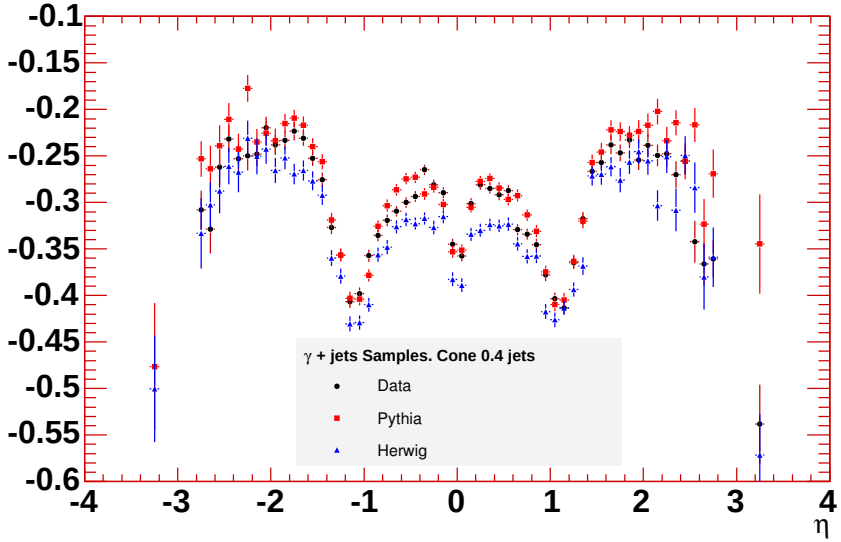

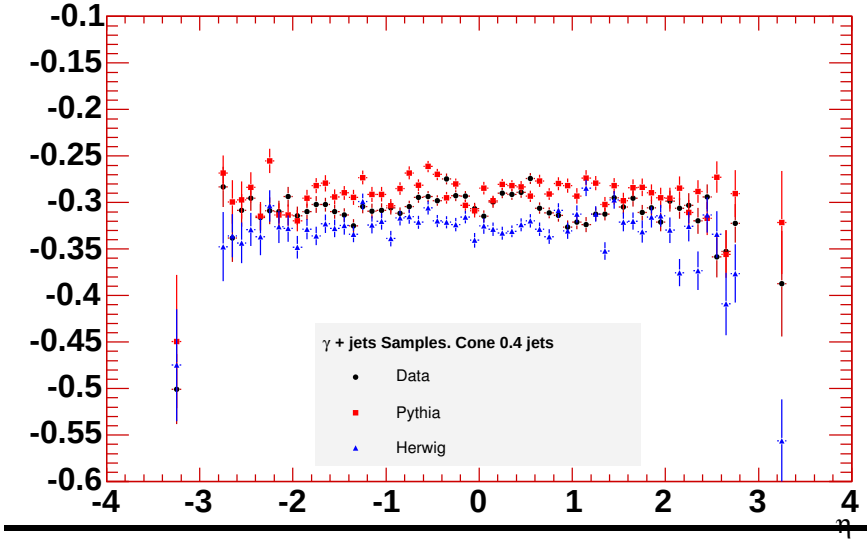

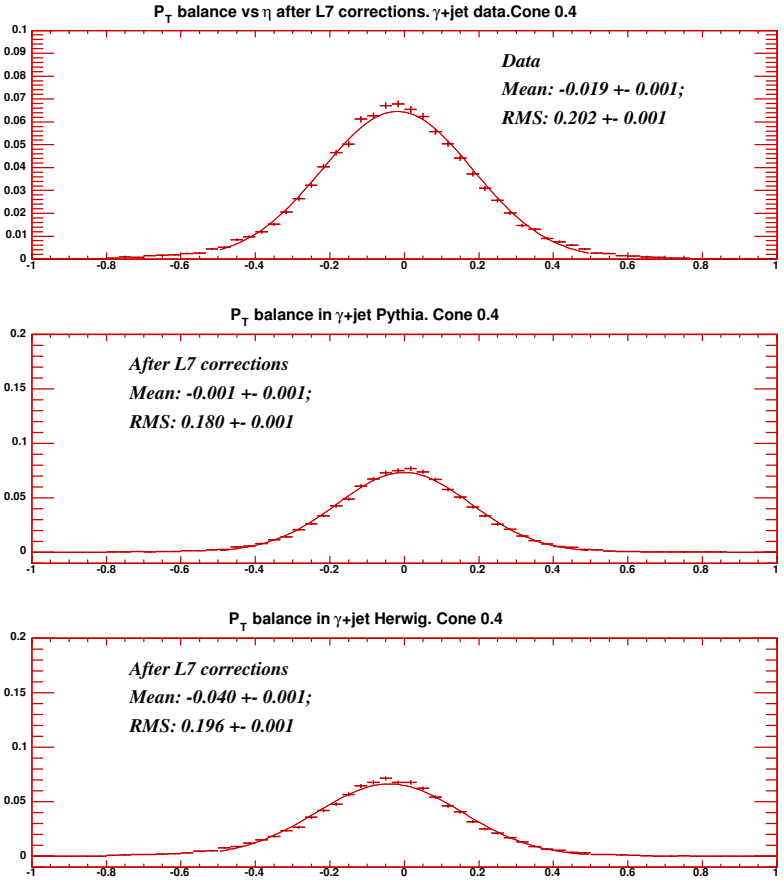

Comparison of data and MC after all corrections.

Figure 10:

6 W and Z^0Production as Archetypes

Let us consider the production of the W and Z^0vector bosons as archetypes of hard processes. Figure 6 shows the dominant diagram and a 'cartoon' of the production process. Both the W and Z are observed in their leptonic decays $W^{\pm} \to l^{\pm}\nu$ and $Z^0 \to \ell\ell$. W

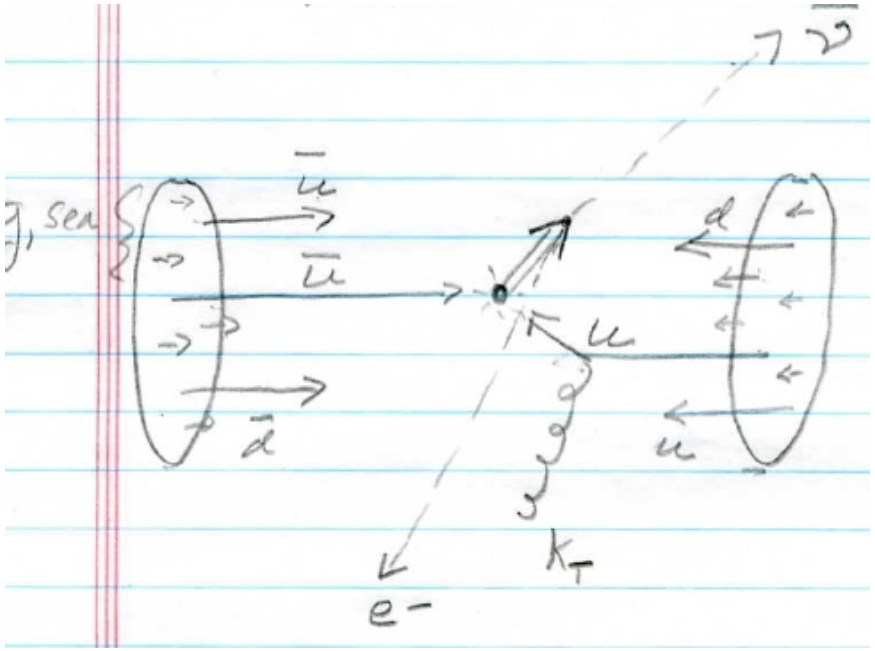

and Z production thus provide a precise measure of the up and down quark parton distribution functions (PDF's).

Since we measure W's and Z's in their leptonic modes, the kinematics of the decay also matter. Consider the W's: they are polarized, as the u and d quarks are light and couple through V-A so quarks have helicity -1 and antiquarks +1. The W decays also by V-A, so the charged leptons come out opposite to the helicity direction. However, the dominant effect, at least at the Tevatron, is that the W is moving in the rest frame, and since the (valence) u quark momentum is generally higher than the (sea) $\bar{d}$ anti-quark; W^+ go in the proton direction, and W^- in the $\bar{p}$ direction (the LHC, being proton-proton, doesn't have this useful asymmetry).

Figure 11 shows the distribution in the difference of e^+ and e^- versus η (pseudo-rapidity) of the electron ($e^\pm$) measured by CDF. The left-hand plot shows the full range as well as the experimental uncertainty band; the right-hand plot shows a comparison with the predictions using the CTEQ6 PDF's. One can see that the PDF's do not fit well.

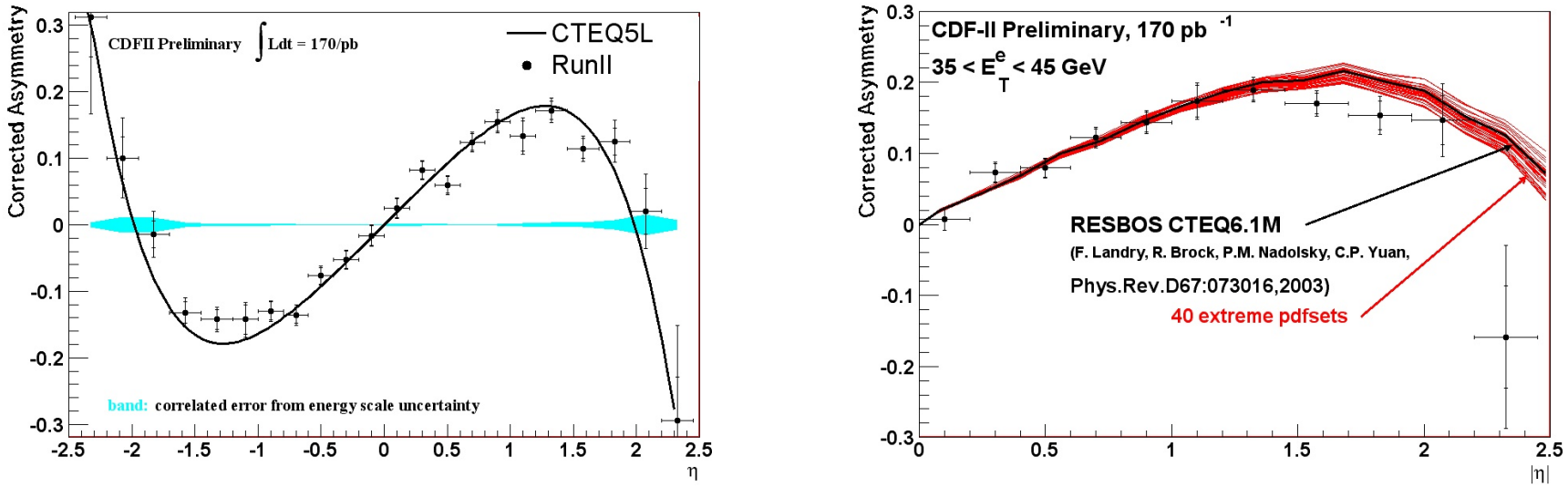

Figure 11: Left: The forward-backward charge asymmetry in $W^{\pm} \to e^{\pm}\nu$ decays plotted versus pseudo-rapidity. The blue error band gives the experimental uncertainty; also shown is the prediction using the CTEQ5L parton distribution functions. Right: The same data, folded around zero in η (remember this is $\bar{p}p$), compared to a prediction using the RESBOS MC generator and the CTEQ6.1M PDF's.

7 'QCD'- Jet Production, Quark and Gluons, ISR, FSR

The dominant feature in the hadron collider landscape is the production of jets- the hard scattering of partons. Figure 7 reproduces two pages from a seminal paper in 1971, when the idea of partons was brand new, by Berman, Bjorken, and Kogut, pointing out that the existence of partons would lead to point-like scatterings and hence high p_T phenomena, including 'cores' (jets). Note the Peyrou plot on the next page...

PHYSICAL REVIEW D VOLUME 4, NUMBER 11 1 DECEMBER 1971

Inclusive Processes at High Transverse Momentum*

S. M. Berman, J. D. Bjorken, and J. B. Kogut†
Stanford Linear Accelerator Center, Stanford University, Stanford, California 94305
(Received 5 August 1971)

We calculate the distribution of secondary particles C in processes $A+B\to C+$ anything at very high energies when (1) particle C has transverse momentum p_T far in excess of 1 GeV/c, (2) the basic reaction mechanism is presumed to be a deep-inelastic electromagnetic process, and (3) particles A, B, and C are either leptons (l), photons (γ), or hadrons (h). We find that such distribution functions possess a scaling behavior, as governed by dimensional analysis. Furthermore, the typical behavior even for A, B, and C all hadrons, is a power-law decrease in yield with increasing p_T, implying measurable yields at NAL of hadrons, leptons, and photons produced in 400-GeV pp collisions even when the observed secondary-particle p_T exceeds 8 GeV/c. There are similar implications for particle yields from e^+-e^- colliding-beam experiments and for hadron yields in deep-inelastic electroproduction (or neutrino processes). Among the processes discussed in some detail are $ll\to h$, $\gamma\gamma\to h$, $lh\to h$, $\gamma h\to h$, $\gamma h\to l$, as well as $hh\to l$, $hh\to\gamma$, $hh\to W$, and $W\to h$, where W is the conjectured weak-interaction intermediate boson. The basis of the calculation is an extension of the parton model. The new ingredient necessary to calculate the processes of interest is the inclusive probability for finding a hadron emerging from a parton struck in a deep-inelastic collision. This probability is taken to have a form similar to that generally presumed for finding a parton in an energetic hadron. We study the dependence of our conclusions on the validity of the parton model, and conclude that they follow mainly from kinematics, duality arguments *à la* Bloom and Gilman, and the crucial assumption that multiplicities in such reactions grow slowly with energy. The picture we obtain generalizes the concept of deep-inelastic process, and predicts the existence of "multiple cores" in such reactions. We speculate on the possibility of strong, nonelectromagnetic deep-inelastic processes. If such processes exist, our predictions of particle yields for $hh\to h$ could be up to 4 orders of magnitude too low, and for $\gamma h\to h$ and $hh\to\gamma$ up to 2 orders of magnitude too low.

I. INTRODUCTION

It is often said that the fundamental reason for building particle accelerators of increasingly higher energy is to probe matter at increasingly smaller distances.[1] However, what is said is often not what is done. The connection between longitudinal momentum and longitudinal distances is, if anything, the opposite; as the energy increases the important longitudinal distances increase.[2] The connection between transverse momentum and transverse distances, indeed, is likely to be that given by the Heisenberg uncertainty relations. Nevertheless, the extensively studied two-body and quasi-two-body processes are dominated by impact parameters of order 1 F, independent of incident energy. Distributions of secondary particles in strong interactions are dominated by low $p_T\lesssim 0.5$ GeV/c corresponding again to the same distances ~1 F, of the order of the physical extension of the particles. Indeed, these distributions fall so precipitously with increasing p_T, with empirical fits typically of the form e^{-ap_T} or $e^{-bp_T^2}$, that one is not sure whether there will be measurable production of very high p_T (>5 GeV/c) particles in strong-interaction processes.

On the other hand, high-energy tests of pure quantum electrodynamics do exhibit a sensitivity to small distances, and more recently deep-inelastic electroproduction experiments and high-energy neutrino processes have opened up a new class of processes which indeed appear to be sensitive to small transverse distances. It is the purpose of this paper to explore as systematically as possible the implications of this class of processes in hadron-hadron and other kinds of collisions. Specifically, we examine inclusive processes initiated by high-energy hadron, photon, or lepton projectiles in which the observed particle has large transverse momentum, i.e., greater than several GeV. If the exponential transverse-momentum dependence associated with pure hadronic interactions remains valid for somewhat larger values of transverse momentum, then the differential cross sections will decrease sufficiently so that electromagnetic interactions could become important. In fact, we find that the known deep-inelastic electromagnetic mechanism is sufficient to provide a population of the high-p_T region of phase space which falls off (at sufficiently high energy)

roughly as a power, not as an exponential of p_T.

In order to estimate the contribution to inclusive processes from an electromagnetic effect, we use an extension of the parton model[3] where the basic process is the electromagnetic interaction between the constituent partons. While the parton model is, to be sure, of dubious quality, we believe that most of our qualitative conclusions follow (within, say, a factor 10 accuracy) from two general considerations. These are, first, the over-all kinematics, and second, the presumption that the mean multiplicity for these high-p_T processes grows slowly with increasing incident energy, final $p_\parallel$ and p_T, more slowly, say, than a power of these variables. This will be discussed in more detail in Sec. IV and in the Conclusion of the paper.

To compare with the extrapolations of the hadronic reactions, we consider as an example the inclusive process $A+B\to C+$anything where A, B, and C are hadrons. The graphs in Fig. 1 compare our parton-model calculation of the differential cross section to observe particle C at 90° in the c.m. system with a conservative extrapolation[4] ($d\sigma/dp_T^2 \sim e^{-6p_T}$) of the purely hadronic background for an NAL condition of $s=800$ GeV^2. In particular, the comparison shows that in the neighborhood of $p_T \approx 5$ GeV/c there should be an abrupt flattening of the slope of the observed cross section. For smaller angles this could occur at an even smaller value of p_T.

Of course, the extrapolation in p_T of the form e^{-6p_T} to such large values could be quite erroneous. On the other hand, the electromagnetic process *must* be present and thus our results based on electromagnetic contributions may be viewed as a *lower bound* on the real cross sections at large p_T.

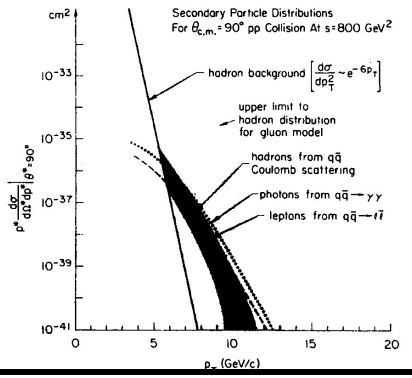

FIG. 1. Secondary-particle distributions as calculated in the parton model and compared to diffractive backgrounds for typical NAL conditions.

It may even be that the electromagnetic contribution to such a process is never dominant. Such a case exists in the model of Wu and Yang[5] which describes elastic proton-proton scattering data reasonably well. In the Wu-Yang model, partons interact strongly with each other via a current-current coupling, such as would arise from exchange of a $J=1$ "gluon." If such an analogy to the vector electromagnetic interaction should hold true for the inelastic case,[6] then because of the slow falloff with respect to q^2 of the electromagnetic structure function a similar weak dependence would be expected for the analogous large-momentum-transfer hadronic reaction. In this case we would expect similar distributions to the examples given here, but increased in order of magnitude by a factor of $\lesssim 10^4$ since the factor of α^2 would be absent. This emphasizes our point of view that the purely electromagnetic processes provide only lower limits to the real differential cross sections.

However, while the interpretation of inelastic electron scattering supports the fact that the photon-parton couplings exist, only vague speculations can be made regarding the pure strong parton vertices. We will thus confine ourselves to only those processes where the scattering vertices occur through photon emission or absorption and thus expect only a lower limit on the possible size of these processes.

In any case, this lower limit shows a reasonable magnitude for the expected large-transverse-momentum cross section, indicating that study of these processes is not only of considerable theoretical interest but also definitely within the realm of experimental feasibility.

The main body of this paper is divided into four sections. In Sec. II we introduce the parton model used in the calculations and generalize the notion of deep-inelastic processes to encompass a wide class of scattering processes. Our parton model is specified by two differential probabilities: The first, called $F(x)$, describes the constitution of an energetic hadron as an ensemble of partons. The second, $G(x)$, describes the decay of a parton isolated in phase space into a system of hadrons. The existence and properties of G are motivated on the basis of our experience with hadron-hadron processes. Two forms for G are proposed which should bracket the true function which will be measured in colliding-beam experiments.

In Sec. III we sketch the calculations of the inclusive differential cross sections of interest. We find that they can be written in a universal form consisting of two factors, $4\pi\alpha^2/p_T^4$ characteristic of single-photon exchange and a form factor

isfy (2.4). This approximation should be sufficient for the kind of order-of-magnitude estimations of interest here.

We test the sensitivity of our calculations to the explicit choice of the function $G(x)$ by considering a second possibility of the form $G(x)=2(1-x)$ which is also commensurate with our intuition, the sum rules and the power-law nature of $G(x)$ near the endpoint $x=1$. In the numerical estimates here this choice can yield values nearly an order of magnitude larger for our expected cross sections and thus gives an estimation of the sensitivity of our results to $G(x)$.

We will see in Secs. III and IV that if one accepts our parton model, the function $G(x)$ can be directly related to the colliding-beam experiments and to electroproduction of hadrons. The data which will soon be available will eliminate our uncertainty concerning the character of $G(x)$.

To give experimental support for the existence of the function $G(x)$ as well as to test for the presence of strong parton-parton interactions, it is important to search for other experimental consequences of deep-inelastic processes. We briefly digress to discuss what general characteristics they would probably have. Consider proton-proton scattering in the center-of-mass frame under CERN intersecting storage ring (ISR) conditions. In phase space a typical initial-state parton distribution is shown in Fig. 4(a). Suppose the partons with longitudinal momenta -9 and $+16$ GeV/c suffer a deep-inelastic scatter through 90° in their center-of-mass frame, producing intermediate state (b) in Fig. 4. This state may further evolve through final-state interactions which predominantly would not be expected to also be deep-inelastic. At the very minimum, the isolated high-p_T partons will communicate with the "wee" partons by cascade emission of partons. If only low-p_T mechanisms are involved in the cascade, the resultant parton four-momenta (approximately null) will be proportional to the parent-parton four-momentum. The result is Fig. 4(c). The hadron distribution would also be similar to Fig. 4(c), and the loci of all phase points in momentum space of secondary hadrons in such an event would lie along three straight lines with perhaps a dispersion Δp_T of order 0.3 GeV/c. This is, in cosmic-ray parlance, the phenomenon of "multiple cores." Measurements of the total energy of the cores and their angles determine the center-of-mass energy of the parton-parton system and also the center-of-mass scattering angle. Such information would shed much light on the nature of the most basic elements of strong-interaction dynamics, despite the fact that the parton charge, spin, etc., are not directly observed.

III. CROSS SECTIONS FOR THE VARIOUS PROCESSES

A. Kinematics

In the limit of high energy and high transverse momentum, we assume that we may neglect all hadron masses, parton masses, and parton or hadron transverse-momentum exchange in the structure factors F and G, as discussed in Sec. II. Thus no intrinsic dimensions remain and all cross sections we discuss will exhibit a scaling behavior. It behooves us to introduce scaling variables in terms of which the cross-section formulas are concisely written. With the notation of Fig. 5, we choose

$$x_1 = -\frac{(p_b-p_c)^2}{(p_a+p_b)^2} = \frac{-u}{s}, \qquad x_2 = -\frac{(p_a-p_c)^2}{(p_a+p_b)^2} = \frac{-t}{s}, \tag{3.1}$$

which satisfy

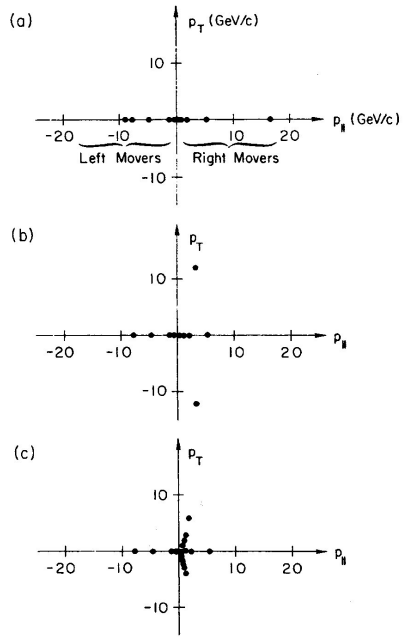

FIG. 4. A momentum-space visualization of hadron-hadron deep-inelastic scattering occurring in three steps.

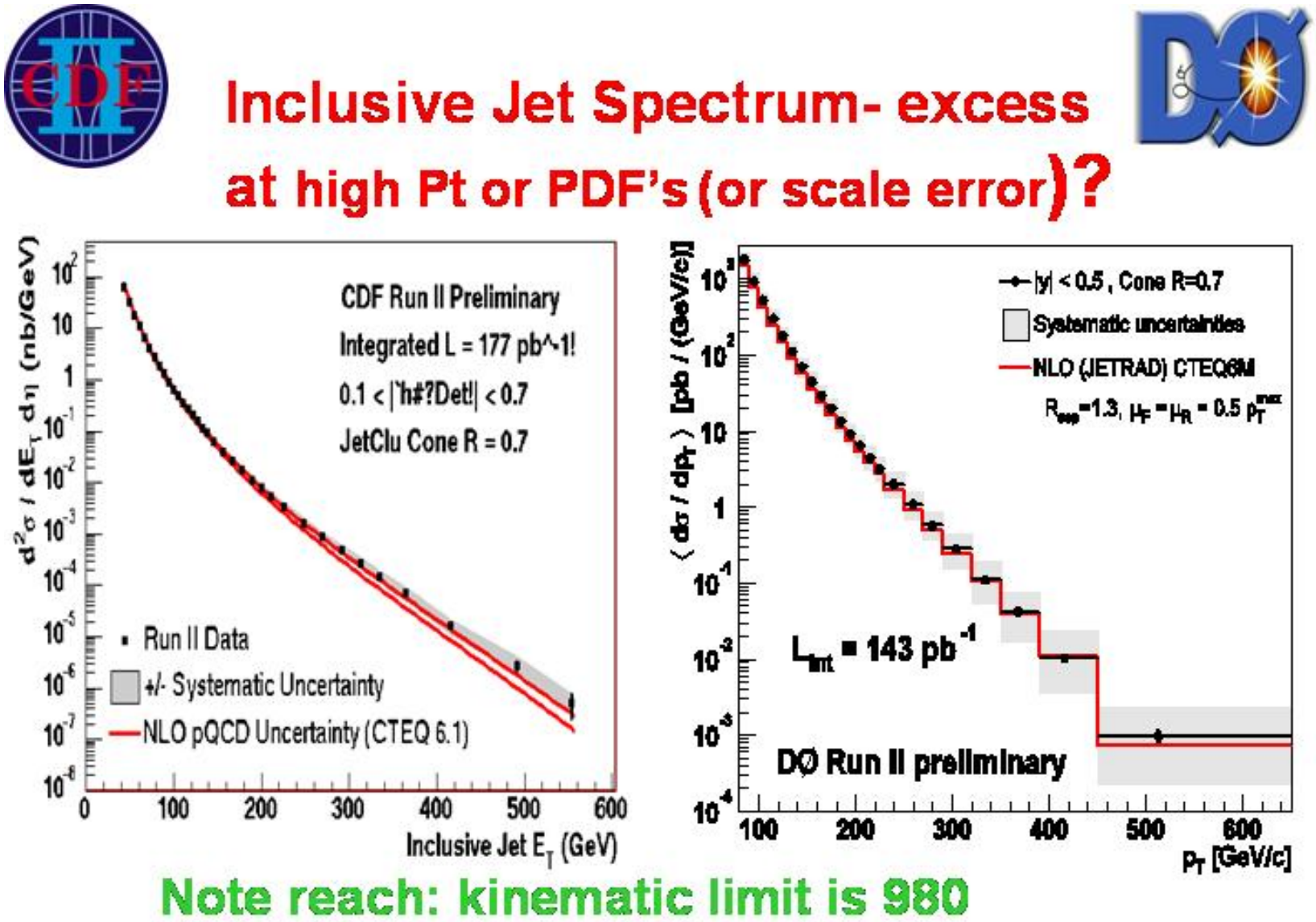
Inclusive Jet Spectrum- excess
at high Pt or PDF's (or scale error)?
CDF Run II Preliminary
Integrated L = 177 pb^-1!
0.1 < |h#?Det!| < 0.7
JetClu Cone R = 0.7
Run II Data
+/- Systematic Uncertainty
NLO pQCD Uncertainty (CTEQ 6.1)
d²σ / dE_T dη (nb/GeV)
Inclusive Jet E_T (GeV)
|y| < 0.5, Cone R=0.7
Systematic uncertainties
NLO (JETRAD) CTEQ6M
R_sep=1.3, μ_F = μ_R = 0.5 p_T^max
L_int = 143 pb^-1
DØ Run II preliminary
⟨ dσ / dp_T ⟩ [pb / (GeV/c)]
p_T [GeV/c]
Note reach: kinematic limit is 980

Figure 12:

High Et jets- comparison to expectations

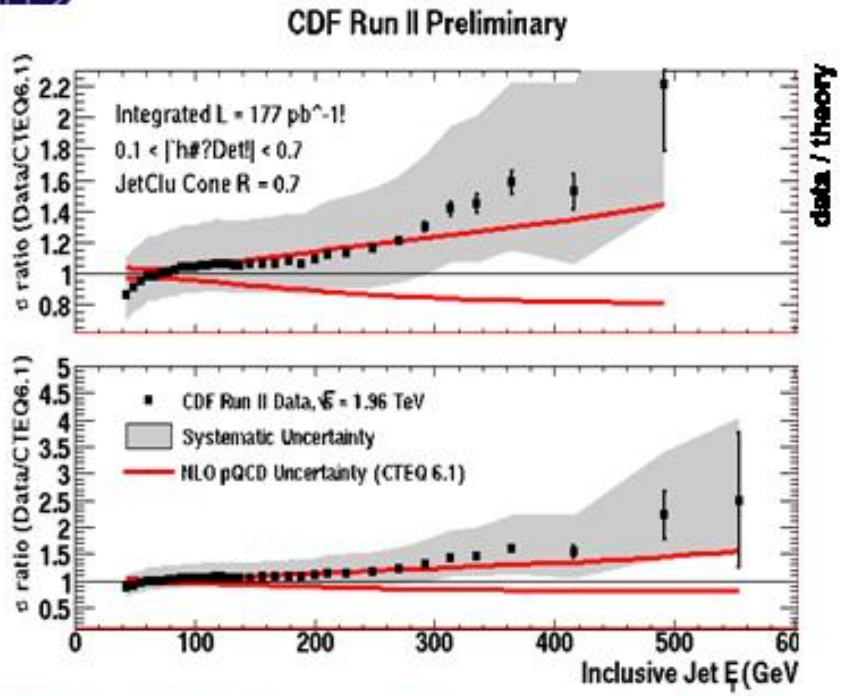

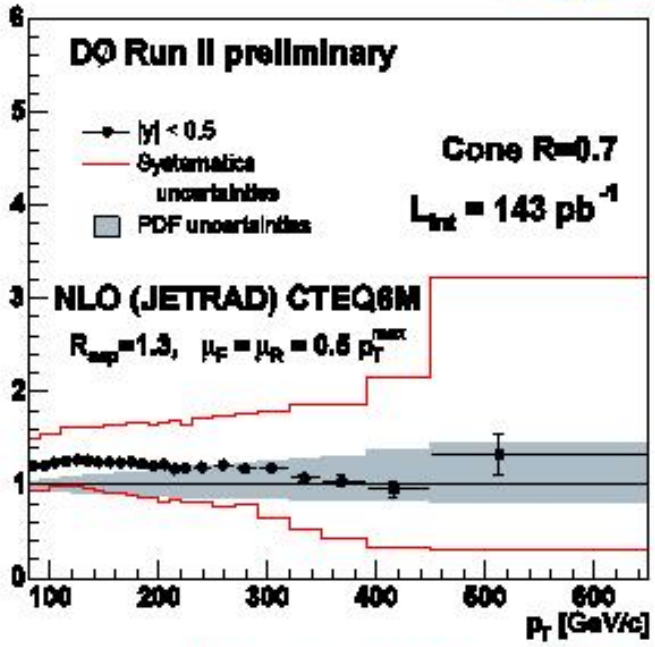

Wish List Item: Answer to Q: Can one calibrate highest Et jets against sum of several lower Et jets? E.g. take events with only 1 jet in hemisphere and max jet in opp. hemisphere < 60% of 1st jet; balance sums in 2 hemispheres (i.e. a bootstrap calibration.)

Figure 13:

Measuring Jets

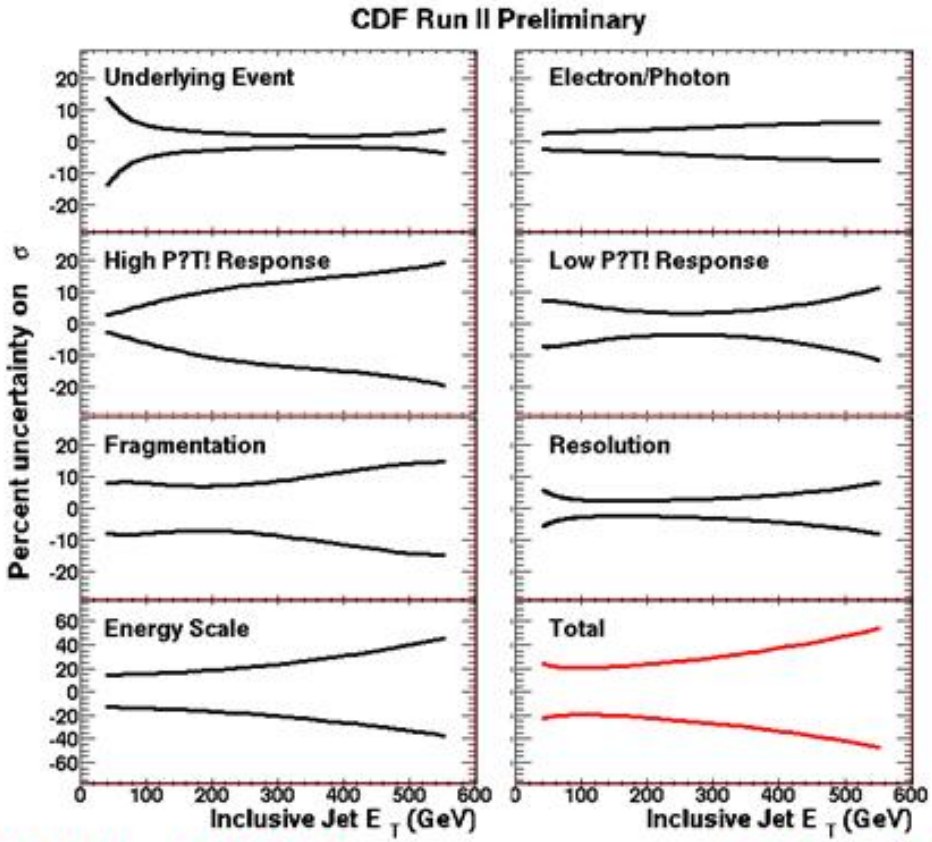

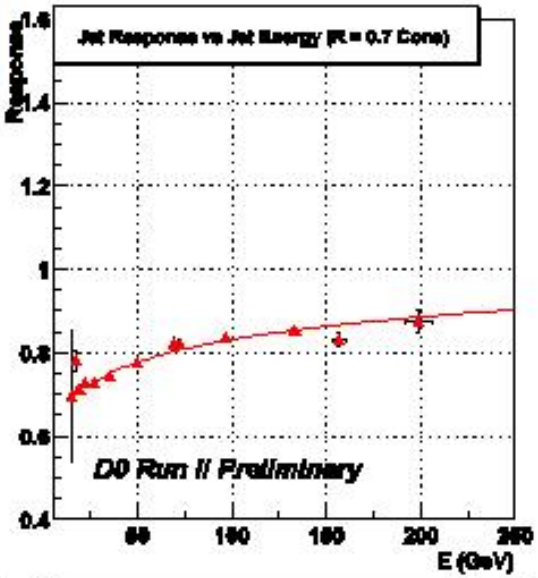

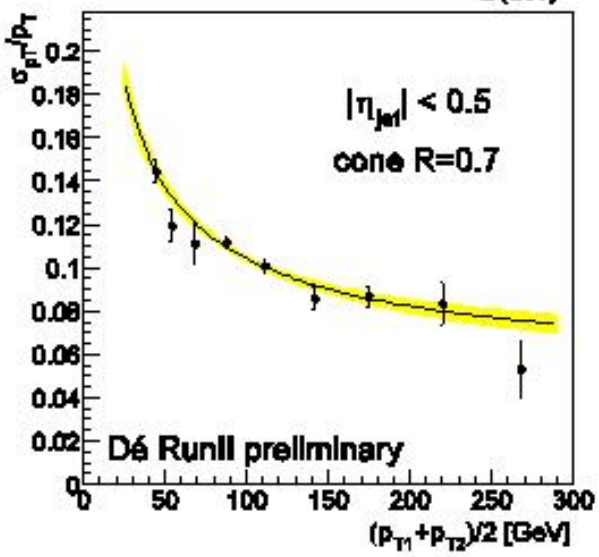

Wish List Item: comparable plots from both experiments (!).

Figure 14:

Jet energy scale is critical to top mass measurement

Balance in Pythia gamma-jet

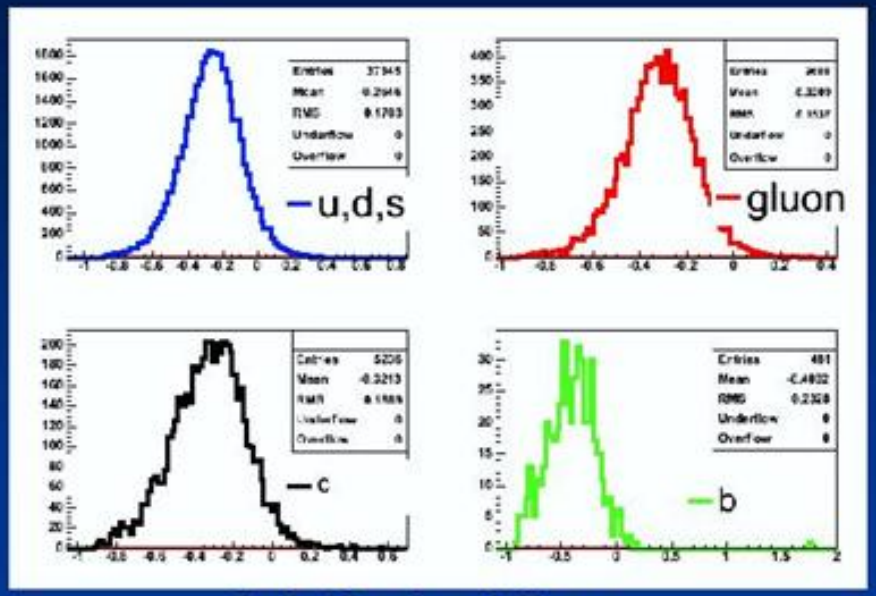

Fbal = (Jet-photon)/Photon:
E_T(central photon)>27 GeV
E_T(2nd jet)>3
delphi(1st jet, photon)>3.0

Un-Ki Yang
Adam Gibson

B-jets contribute most to mass (don't have W mass constraint)…

Promising Idea:

Balance photon and b-jets to calibrate response

Wish List Item: Answer to Q: What are the theoretical limitations on the ratio of gamma-b(c)/gamma-jet balancing?

Figure 15:

8 The $M_{Top} - M_W$ Plane and the Higgs Mass

8.1 Motivation

The top quark is remarkable for its physics and useful as a tool for calibration. It may also be a window into the world of heavy weakly-interacting particles (such as a Higgs of one sort or another) in that it is produced strongly (i.e with coupling $O\alpha_s$) in pairs, but due to its strongly-conserved flavor quantum number (top-ness), has to decay electro-weakly. Due to radiative corrections, the masses of the W, Z, Higgs, and top quark are related in the SM; precise measurements of the W and top quark masses determine the predicted Higgs mass.

8.2 What limits the precision on the W mass and the top mass measurements?

Figure 18 gives the history of the uncertainty on the W mass as a function of the square-root of luminosity. The statistical uncertainty is expected to scale as $\int \mathcal{L}dt^{-1}$. The systematic uncertainties will be discussed below when we get to the measurement of the W mass; however it is interesting to note that since the systematics are studied with data, they also seem to scale with luminosity. If the control of systematic uncer-

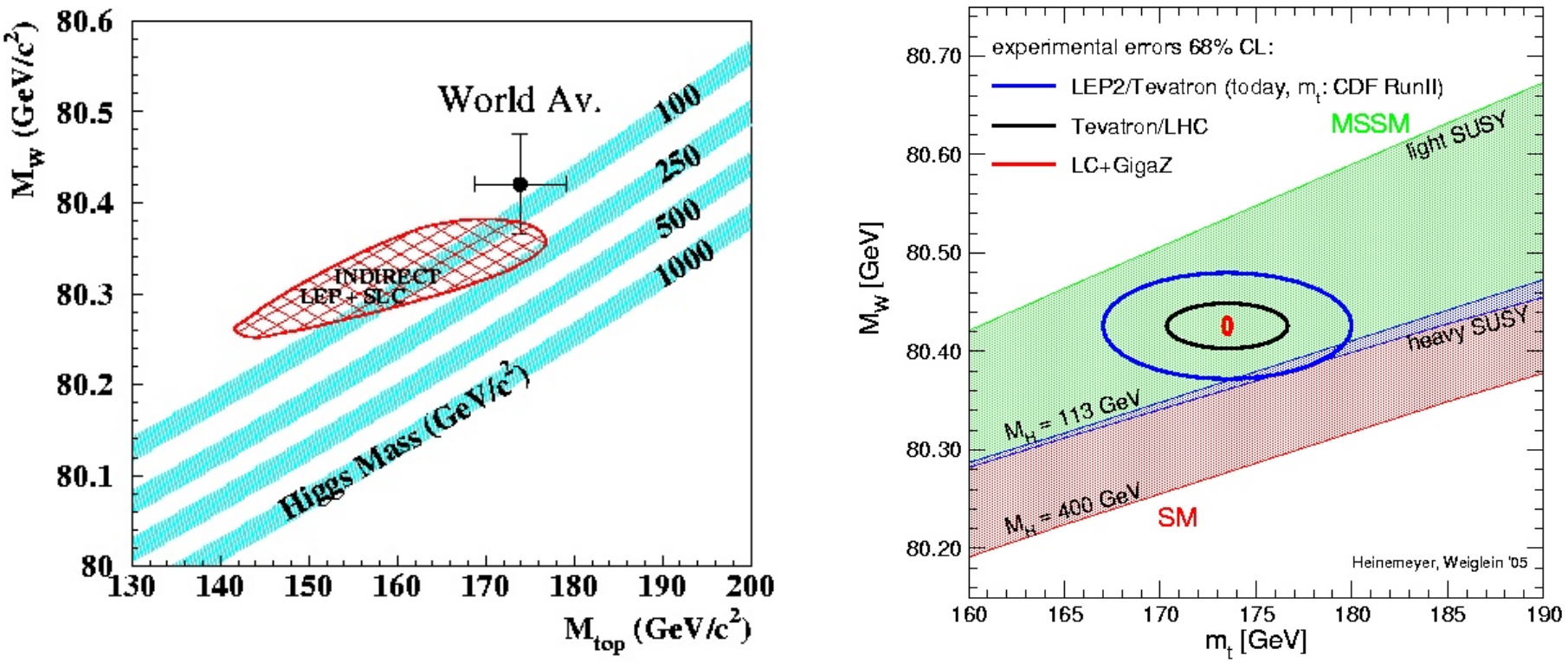

Figure 16: Left: The M_W vs M_T plane as of March 1998. Right: The M_W vs M_T plane as of the summer of 2005. Note the difference in the scales of the abscissas.

tainties continues to scale with statistics as $\int \mathcal{L}dt^{-1}$ the Tevatron can do as well as LHC projections [**?**], and with very different systematics.

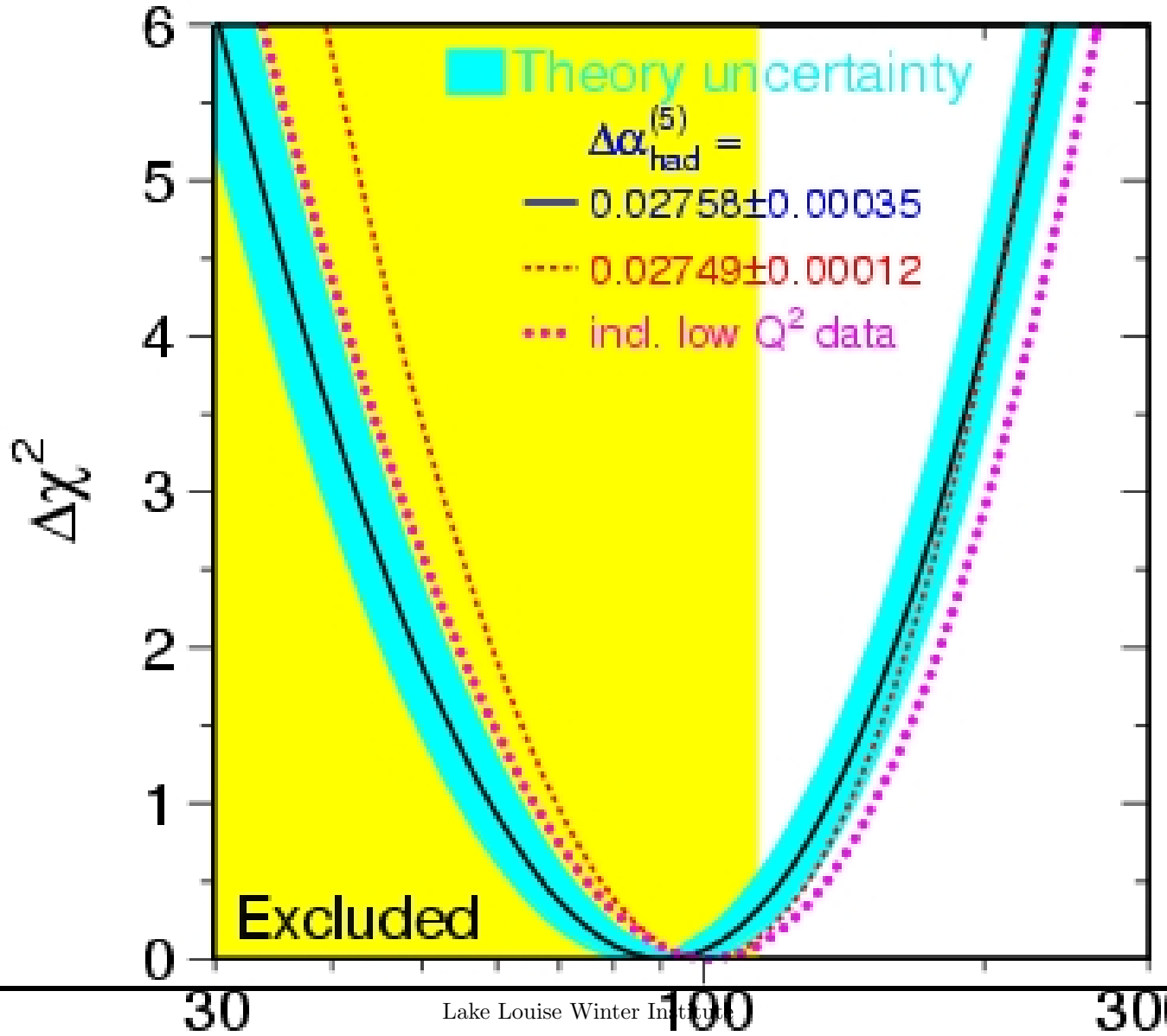
Theory uncertainty
$\Delta\alpha^{(5)}_{had}$ =
0.02758±0.00035
0.02749±0.00012
incl. low Q^2 data
$\Delta\chi^2$
Excluded
0
1
2
3
4
5
6
30
100
300

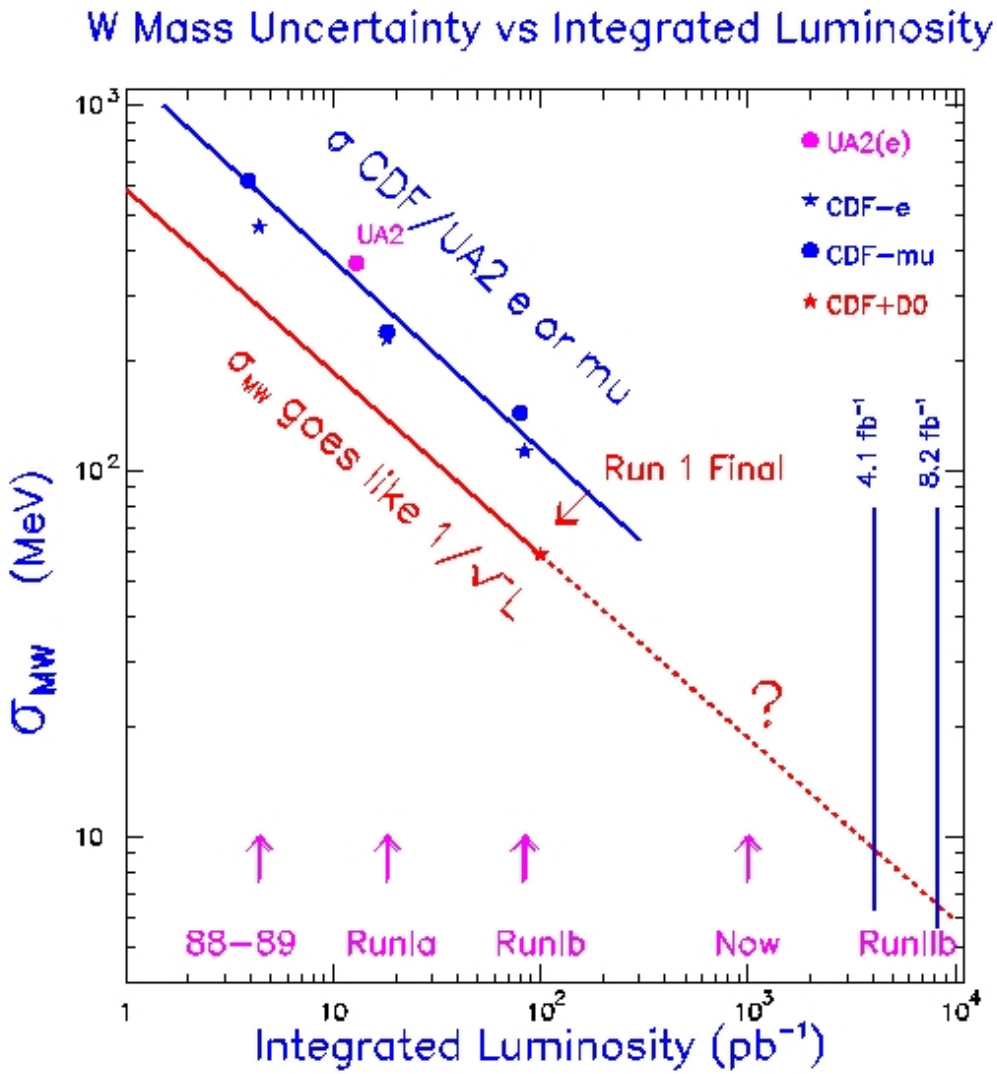

Figure 18: The total uncertainty on the W mass as measured at the Tevatron, versus integrated luminosity. If the control of systematic uncertainties continues to scale with statistics as $\int \mathcal{L}dt^{-1}$ the Tevatron can do as well as LHC projections, and with different systematics.

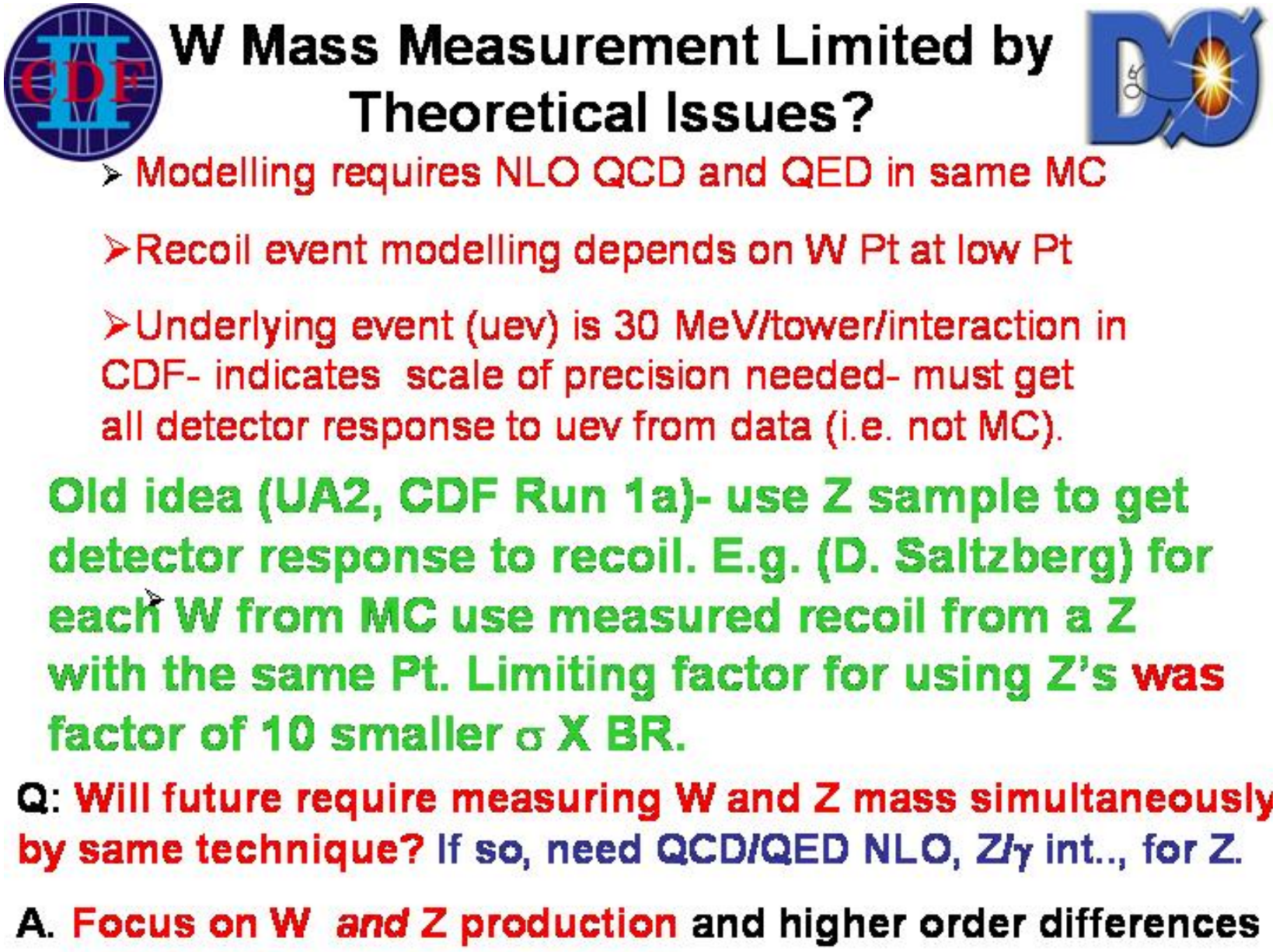
W Mass Measurement Limited by Theoretical Issues?
CDF
DØ
Modelling requires NLO QCD and QED in same MC
Recoil event modelling depends on W Pt at low Pt
Underlying event (uev) is 30 MeV/tower/interaction in CDF- indicates scale of precision needed- must get all detector response to uev from data (i.e. not MC).
Old idea (UA2, CDF Run 1a)- use Z sample to get detector response to recoil. E.g. (D. Saltzberg) for each W from MC use measured recoil from a Z with the same Pt. Limiting factor for using Z's was factor of 10 smaller σ X BR.
Q: Will future require measuring W and Z mass simultaneously by same technique? If so, need QCD/QED NLO, Z/γ int.., for Z.
A. Focus on W and Z production and higher order differences

Figure 19:

9 Measuring the Top Quark Mass and Cross-section

I will discuss two specific measurements as pedagogic examples of some specific difficulties (challenges is the polite word) of doing precision measurements - the measurements of the top cross-section and the top mass. The idea is make it possible for you to ask really hard questions when you see the beautiful busy plots that we all usually just let go by. First some basics.

9.1 $t\bar{t}$ Production: Measuring the Top Cross-section Precisely

The prime motivation for a precise measurement of the top cross-section is that new physics could provide an additional source for the production (leading to a larger cross-section than expected) or additional decay channels (leading to a smaller measured cross-section into $\bar{b}$) [**?**]. More prosaically, the cross-section is a well-defined and in-principle easy-to-measure quantity that tests many aspects of QCD and the underlying universe of hadron collider physics- the PDF's, LO, NLO and NNLO calculations, and provides a calibration point for calorimeters and the energy scale (will be a key calibration for LHC). Lastly, and less defensible scientifically, is the uneasy feeling that too low a cross-section (e.g.) means that the top mass is really lighter than we measure, and the crucial

EWK fits and limits on the Higgs mass are thus probably not correct.
Figure 20 shows the dominant diagrams for top production. At the Tevatron (left) the $t\bar{t}$ system, with a mass 400 GeV, samples the structure functions at a typical x given by $< x1x2 >= m^2/\sqrt{s} \eqsim (400/1960)^2$, giving $< x > \eqsim 0.20$, well into the valence quark region. At the LHC, the corresponding value is $< x > \eqsim 0.04$, i.e. in a region dominated by gluons.

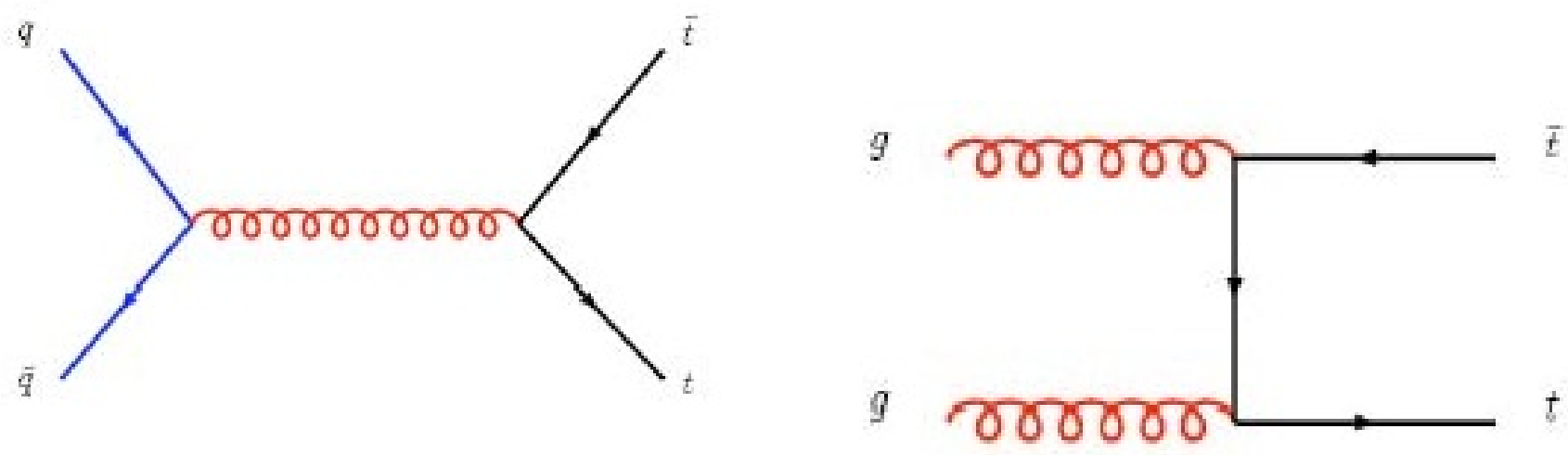

Figure 20: Left: The dominant diagram for $t\bar{t}$ production at the Tevatron; Right: The dominant diagram at the LHC. (from F. Maltoni [**?**]).

9.2 Total Cross-section for $t\bar{t}$ Production: Parsing the CDF and DØ Plots

A brief history of theoretical predictions for σ_{top}:

Theoretical $t\bar{t}$ Cross Section Predictions						
Authors	hep-ph	Date	Order/Resum	PDF	$\sqrt{s} = 1.8$	$\sqrt{s} = 1.96$
Kidonakis+Vogt	0309045	Sep 03	NNLO/yes	CTEQ6M	5.24±.31	6.77±.42
Mangano,Nason, Cacciari,Frixione, +Ridolfi	0303075	Mar 03	NLO/yes	CTEQ6M	$5.9^{+.052}_{-.0.68}$	$6.70^{+.71}_{-.88}$
Kidonakis	0010002	May 01	NNLO/yes NLO/yes	CTEQ5M CTEQ5M	$6.3^{+.1}_{-.4}$ 5.2	$8.1^{+.13}_{-.52}*$ —
PDG (Mangano)	PRD66: 010001	Jun 02	—	—	—	5.13±.38
Bonciani,Catani, Mangano,+Nason	9801375	Mar 98	NLO/yes NLO/no	MRS2 MRS2	$5.06^{+.13}_{-.36}$ $4.87^{+.30}_{-.56}$	$6.53^{+.17}_{-.46}$ ** $6.28^{+.39}_{-.72}$ **
Berger+Contopanagos	9603326	Mar 96	NLO/yes	CTEQ3	$5.52^{+.17}_{-.42}$	$7.17^{+.09}_{-.54}$ **
Laenen,Smith +Van Neerven	9310233	Oct 93	NLO/yes	MRSD′_	$4.95^{+.70}_{-.42}$	$6.39^{+.90}_{-.54}$ **
MadGraph	this note	Jan 04	LO:$Q^2 = M_t^2$	CTEQ5L	—	6.21±0.02
MadGraph	this note	Jan 04	LO:$Q^2 = M_Z^2$	CTEQ5L	—	8.46±0.06

Table 1: A selection of top cross-section predictions. Those numbers tagged by ** have been scaled up to 1.96 TeV from 1.8 TeV by a factor of 1.29 (in many cases the 2.0 TeV crossections are given, but not 1.96). Note that the MadGraph numbers, described in this note, are higher than the NLO and NNLO calculations, which in turn are higher than the 2002 PDG value. This is due to the Q^2 scales, which are M_Z^2 everywhere in this note. Changing the Q^2 scales to M_{top}^2 lowers the crossection to be a little lower than the latest NNLO/NLL calculations.

Both D0 and CDF measure the top cross-section in different channels and sometimes in the same channel by different techniques:

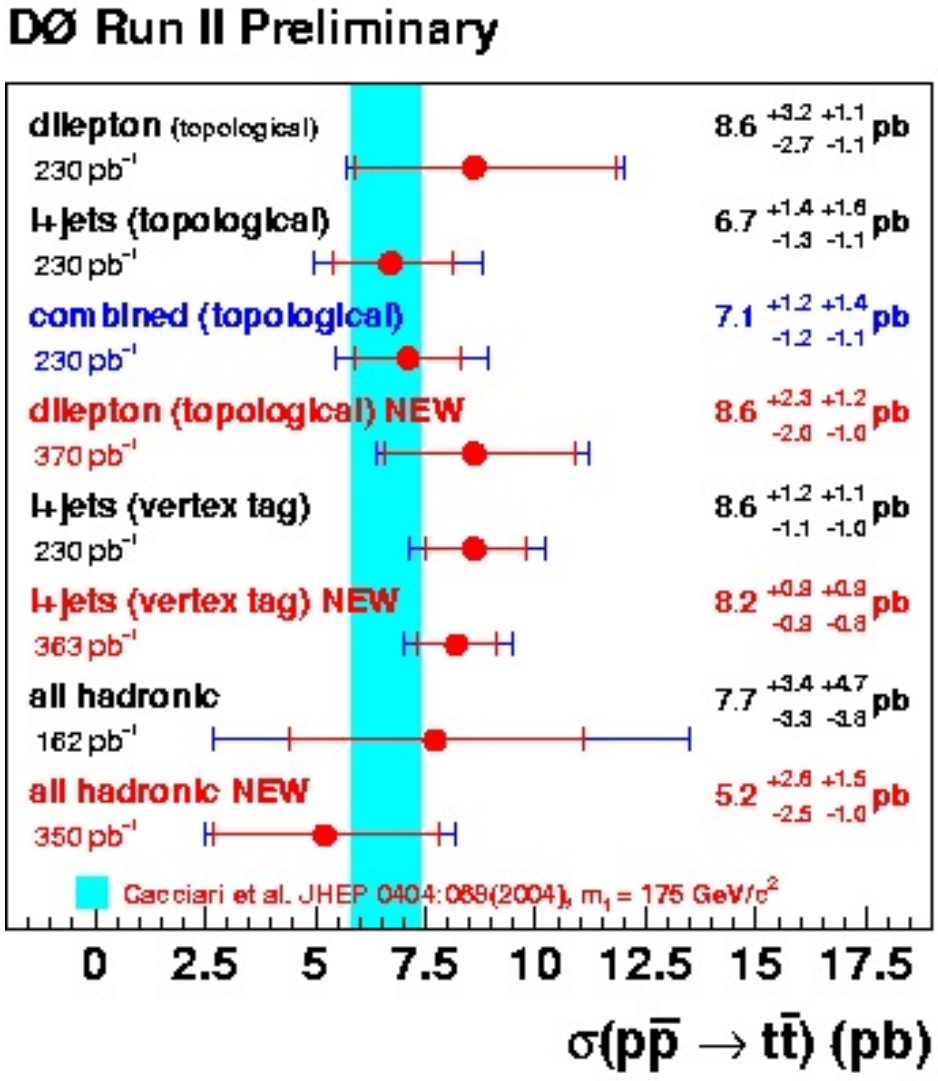

‘200’ pb-1

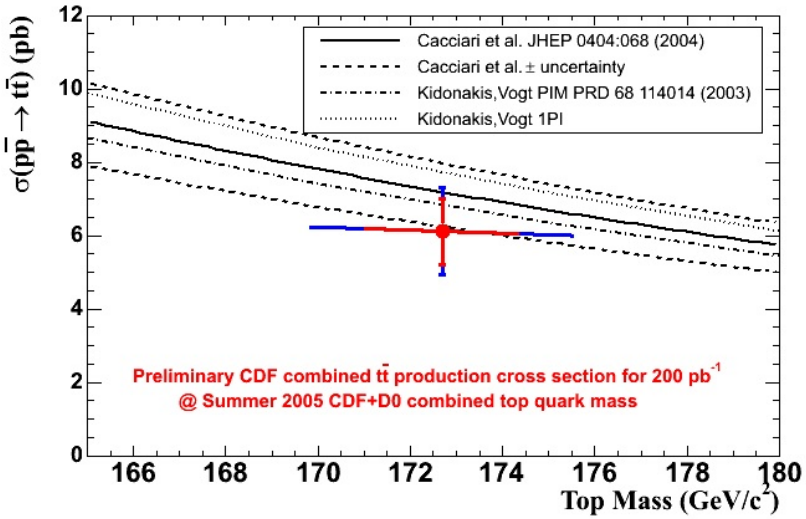

‘350’ pb-1

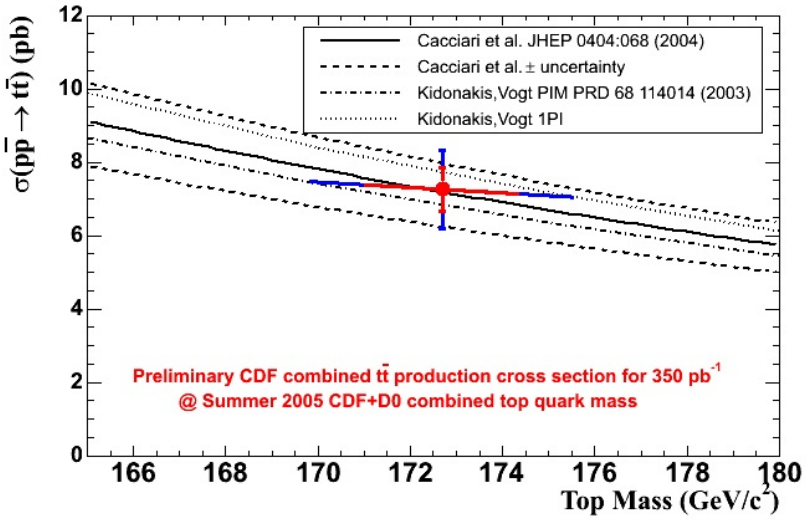

Figure 21: From CDF: The measured and predicted top cross-sections versus mass with approximately 200 pb^{-1}(Left) and now with approximately 350 pb^{-1}(Right).

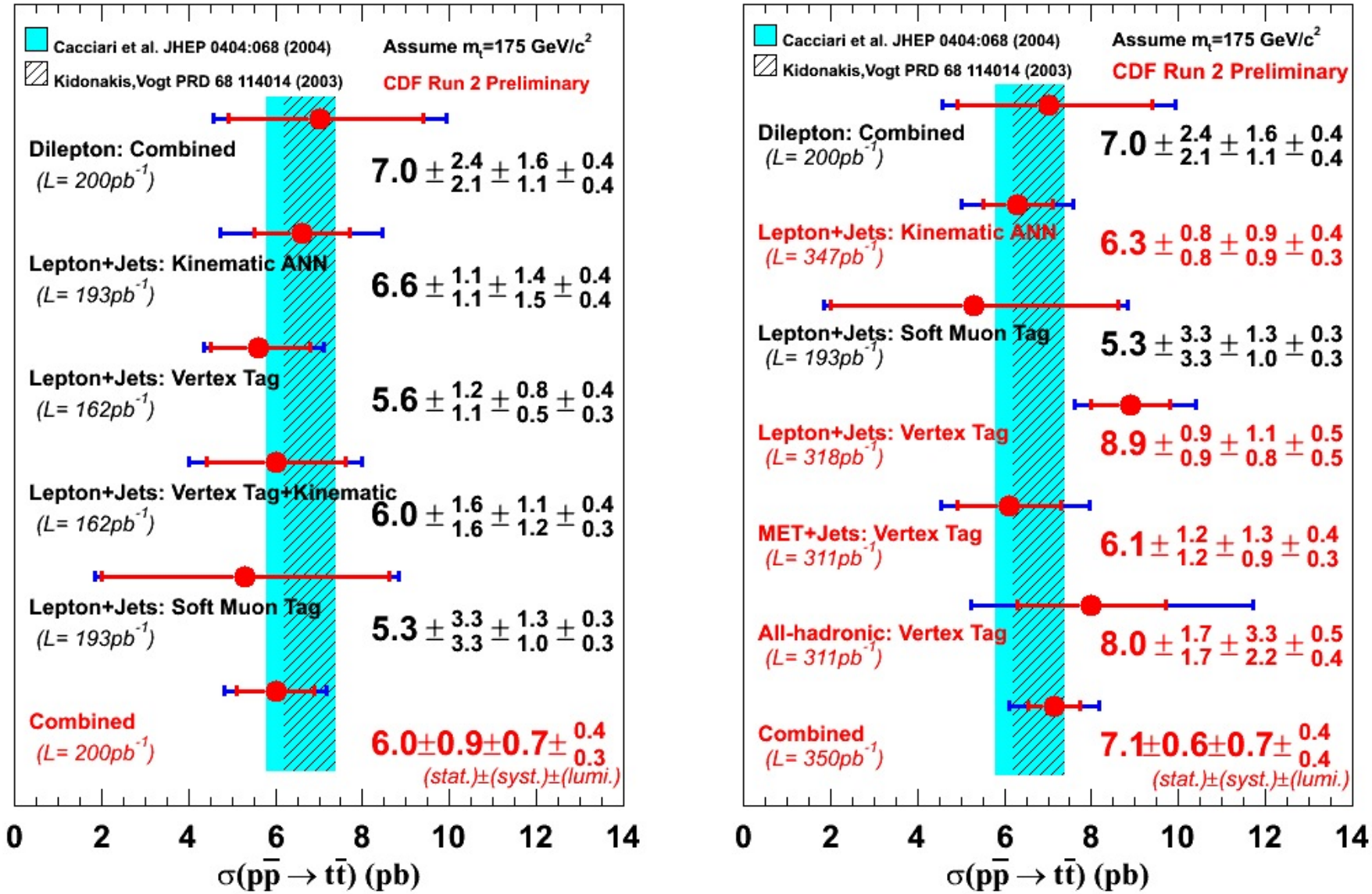

Figure 22: CDF Top Cross-Section Measurements: Left: 200pb^{-1}Right: Left: 200pb^{-1}

9.3 Properties of the $t\bar{t}$ system

The $t\bar{t}$ system is particularly interesting, as there may be new resonances decaying directly into $t\bar{t}$ or new pairs of particles each with a decay into top plus something. Either way there would be a feature in the $t\bar{t}$ mass spectrum and a change in shape in the $t\bar{t}$ p_T spectrum. Figure23

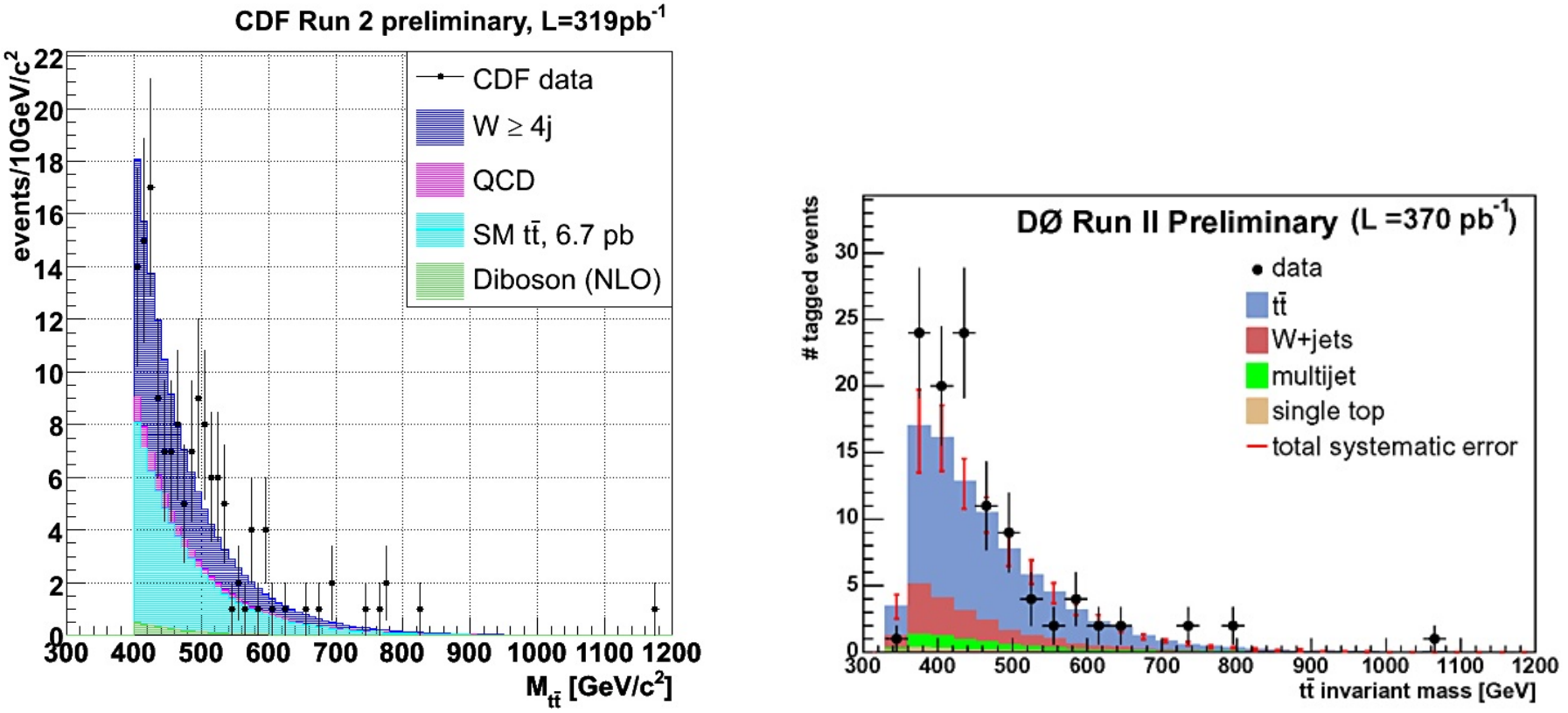

Figure 23: Left: CDF's ttbar mass spectrum from 320 pb^{-1}. Right: The ttbar mass spectrum as measured in 370 $pb^{-1}$by DØ .

Mass Templates for $t\bar{t}$ system:
What is the probability for a lower-mass pair to be reconstructed at a higher mass? Input a mean value for the pair, and look at the output. Abcissa runs from 0 to 1200 GeV.

450 GeV

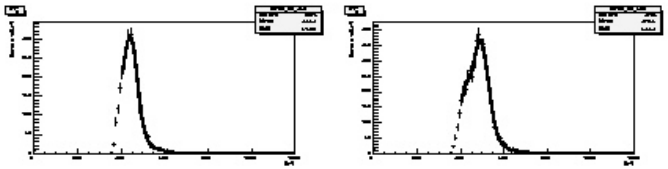

500 GeV

550 GeV

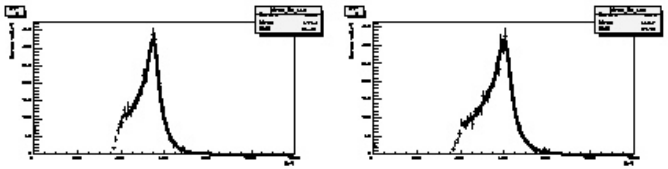

600 GeV

650 GeV

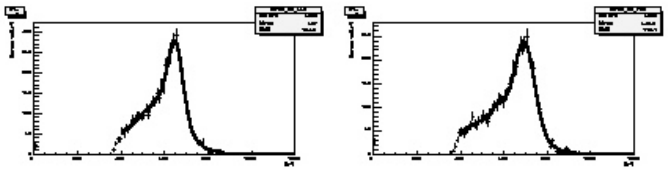

700 GeV

750 GeV

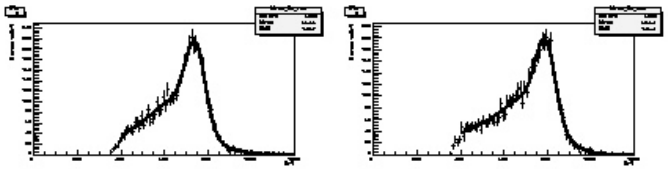

800 GeV

850 GeV

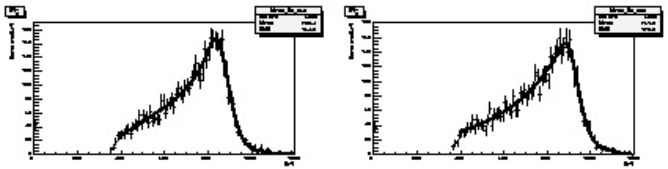

900 GeV

Figure 42: Signal reconstruction

51

9.4 Precision Measurement of the Top Mass

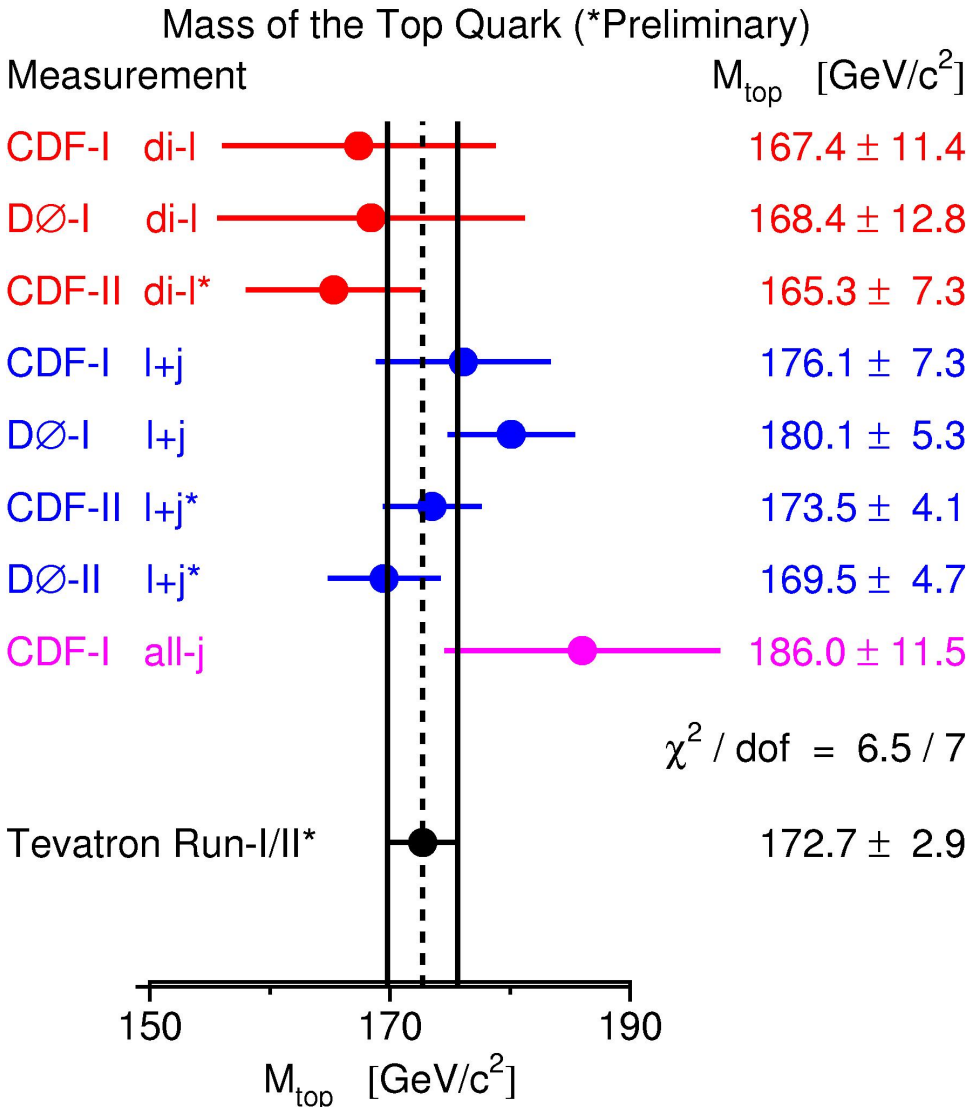

Summary of Top mass Measurements as of July 05. Note the dilepton measurements tend to be systematically lower. A comment- the D0 Run I measurement when analyzed by a different technique (same data, same calibration) moved from 173.3±7.8 to 180.1±5.3. A challenge- how better should we quantify the systematics on data selection and technique?

9.5 CDF Templates in M_{top} and M_{jj} (2D) in Lepton+Jets

CDF Run II Preliminary (318pb $^{-1}$)

Subsample	Number of events m_t	Number of events m_{jj}
2-tag	16	25
1-tag(T)	57	63
1-tag(L)	25	33
0-tag	40	44

The numbers of events in the CDF Template Lepton+Jets analysis.

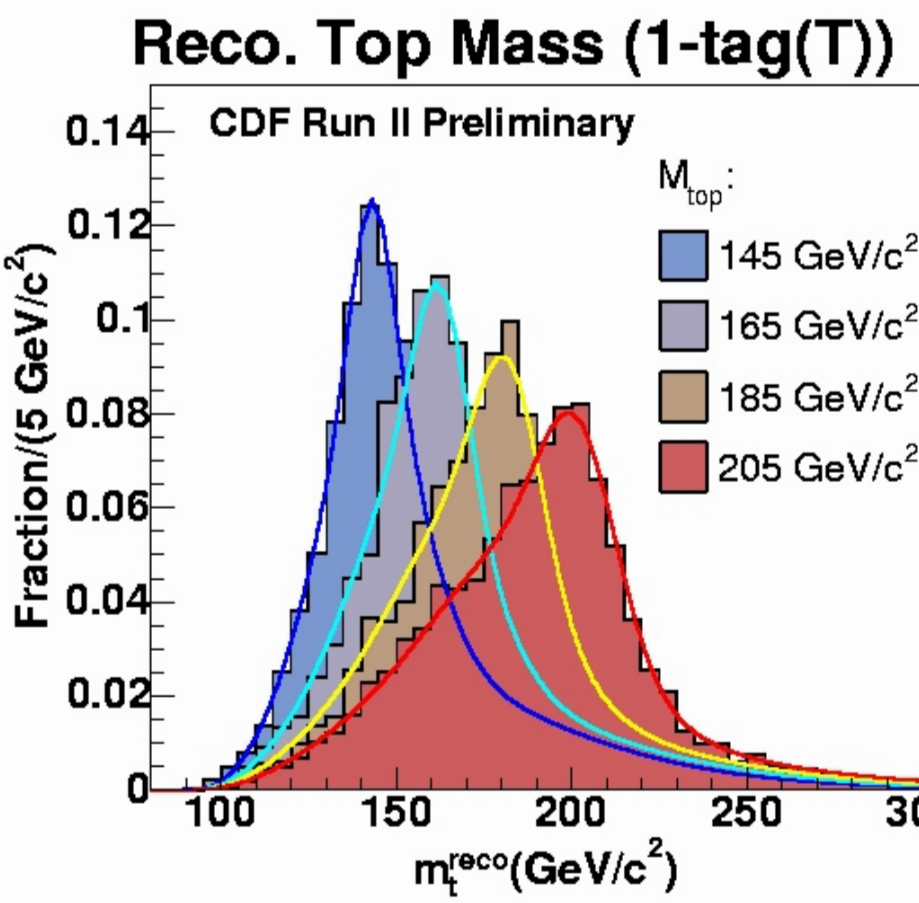

Templates in the Top mass (CDF)

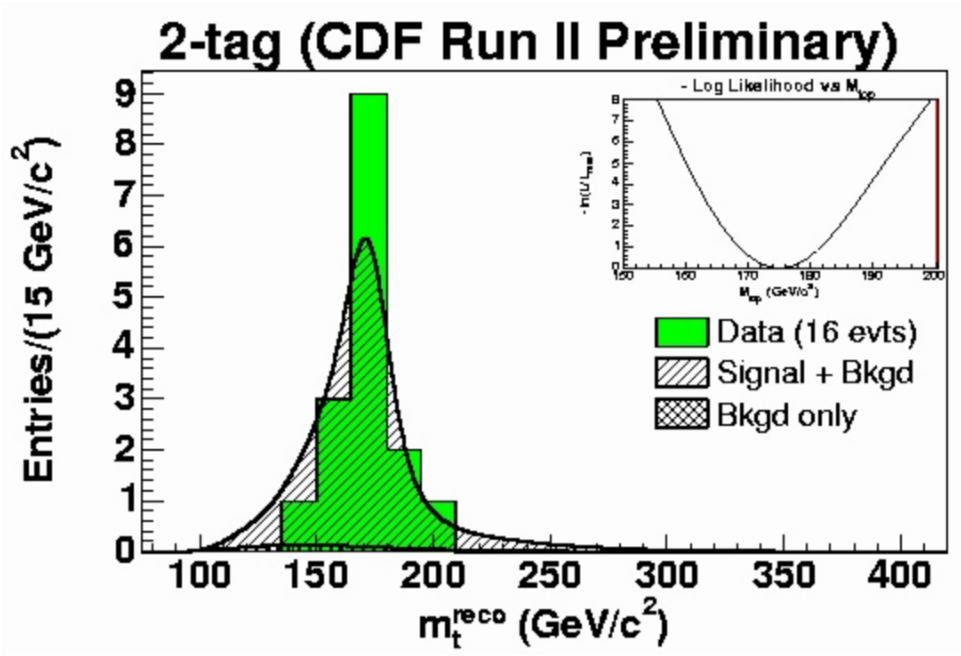

CDF final fit to Mt in lepton+jets

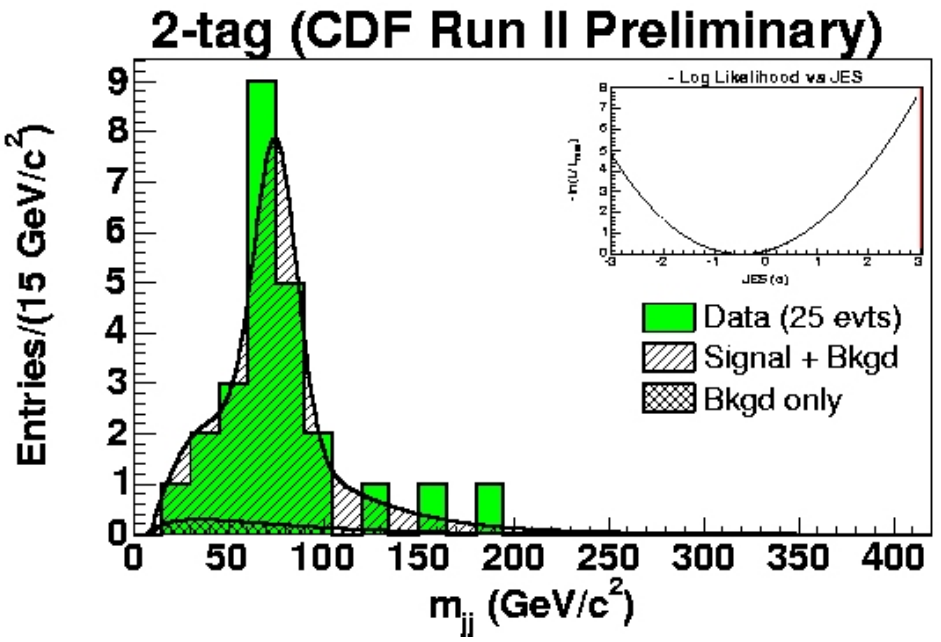

CDF final fit to MW (2-jet invariant mass) in lepton+jets

9.6 DØ Matrix Element Likelihood in M_{top} and M_{jj} (2D) in Lepton+Jets

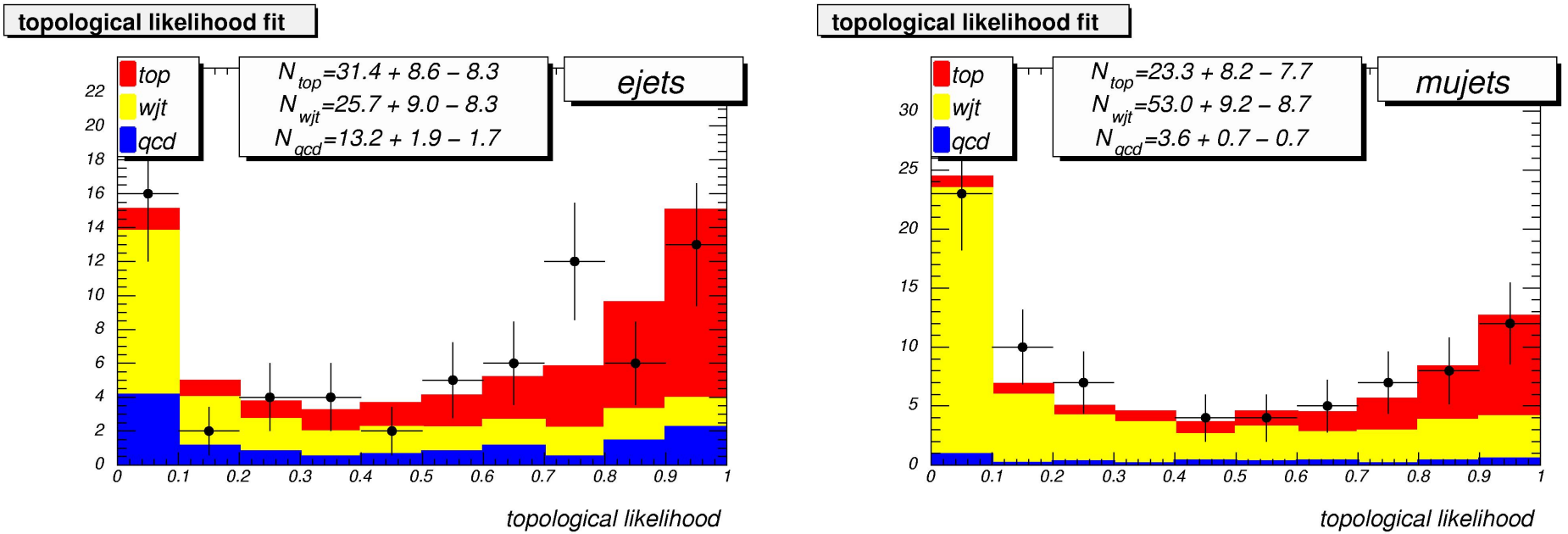

Drawback from more complex methods - often hard to judge by eye how good it looks - takes extra work to make transparent. Net gain in precision- but need simpler parallel analysis for sanity checks.

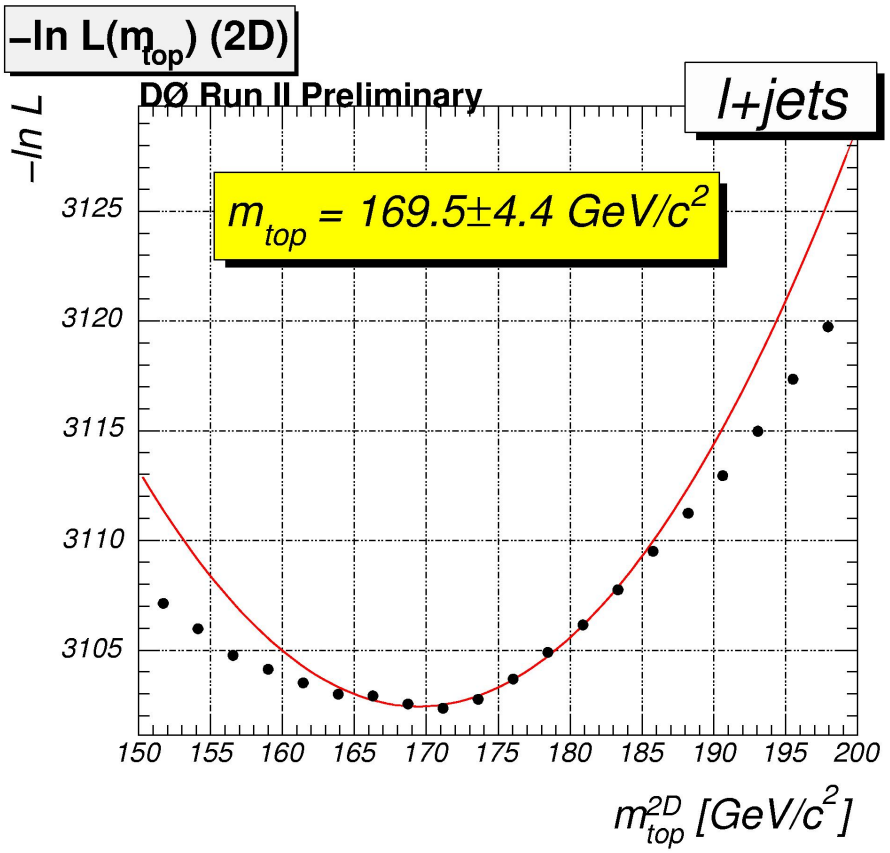

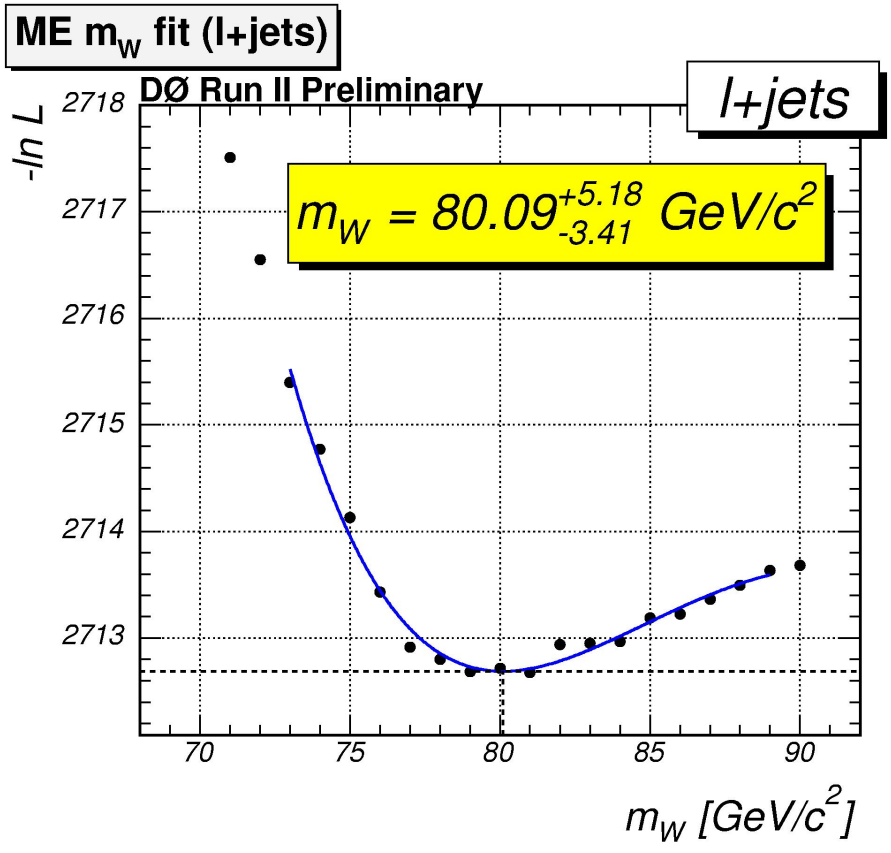

The D0 top and W mass fits in the 2D analysis. Closer to the dilepton number (all with 2 sigma, but...?)

CDF Run II Preliminary

Systematic effect	M_{top} Measurement		JES Cross-Check
	ΔM_{top} (GeV/c^2)	ΔJES (σ)	ΔJES (σ)
b-jets modelling	0.6	0.25	–
Method	0.5	0.02	0.04
ISR	0.4	0.08	0.24
FSR	0.6	0.06	0.24
Generator	0.2	0.15	0.38
PDF	0.3	0.04	0.11
Background shape	0.5	0.08	0.23
MC statistics	0.3	0.05	0.09
B-tagging	0.1	0.01	0.01
M_{top} (JES cross-check only)	–	–	0.36
Total	1.3	0.33	0.68

Uncertainty	ℓ+jets [GeV/c^2]
JES p_T dependence	± 0.7
b fragmentation	± 0.7
b response (l/e)	$+0.87\ -0.75$
signal modeling	± 0.34
background modeling	± 0.32
signal fraction	$+0.50\ -0.13$
QCD contamination	± 0.07
MC calibration	± 0.39
trigger	± 0.08
PDF uncertainty	± 0.07
TOTAL	$+1.7\ -1.6$

TABLE II: Summary of systematic uncertainties.

Summary of First Lecture

- Idea was to introduce key measurements and numbers from previous data so you can look at detailed presentations with a critical eye (discussion)-
- Things to watch for in the following talks on Top, and Electroweak Topics

1. $M_{top} - M_W$ off in (upper) left-field? What is the top mass?
2. 'Bump' in $M_{t\bar{t}}$?
3. σ_{top} and m_{top} consistent with predicted cross-section
4. Systematics- just entering an era of enough data to measure systematics better - new methods, new ideas,...
5. Transparency- can we show more 'under the hood'? (not a black box)-
6. Transparency- can CDF and DØ , and Atlas and CMS, work harder on making comparisons- e.g. plots on same axes and scales...

10 Credits

Talks I have found very useful and/or taken plots from:
Florencia Canelli (UCLA), *QCD and the Importance of Hadron Calibration at the Tevatron*, Feb. 2005, Tev4LHC
Rick Field (Florida) *Jet Physics and the Underlying Event at the Tevatron*, XXXV Symposium on Multiparticle Dynamics, Kromericz, Czech Republic
Kenichi Hatakeyama (Rockefeller), *How to Calibrate Jet Energy Scale*, Coimbra, Portugal; Jan, 2006
Aurelio Juste (FNAL) Lepton-Photon, July, 2005
Cheng-Ju S. Lin, *Heavy Flavor Physics at the Tevatron*, Aspen Winter Conference, Feb. 2006
Fabio Maltoni (CERN, Louvain) *Theoretical Issues and Aims at the Tevatron and LHC*, HCP2005, Les Diableret, Switz., July 2005
Vaia Papadimitriou, *B_S, B_C and b-baryons*, XXXV Symposium on Multiparticle Dynamics, Kromericz, Czech Republic
Eric Varnes (Arizona), *Measurement of Top Quark Decay Properties at Run II of the Tevatron*, Top2006, Coimbra, Portugal; Jan, 2006
Evelyn Thompson (Penn) *Experimental Methods*, Top2006, Coimbra, Portugal; Jan,

2006
Carlos Wagner (ANL,UC) EFI Presentation, February 2006

Many thanks to: Eric Brubaker, Robin Erbacher, Ivan Furic, Chris Hays, Matt Herndon, John Hobbs, Joey Huston, Steve Levy, Andrei Loginov, Ashutosh Kotwal, Vaia Papadimitriou, Jon Rosner, Jim Strait, Evelyn Thompson, Carlos Wagner